arXiv:1511.01414v1 [math.DS] 4 Nov 2015

Global bifurcation diagram of steady states of systems of PDEs via rigorous numerics: a 3-component reaction-diffusion system

Maxime Breden * Jean-Philippe Lessard† Matthieu Vanicat ‡

January 2013

Abstract

In this paper, we use rigorous numerics to compute several global smooth branches of steady states for a system of three reaction-diffusion PDEs introduced by Iida et al. [J. Math. Biol., **53**, 617–641 (2006)] to study the effect of cross-diffusion in competitive interactions. An explicit and mathematically rigorous construction of a global bifurcation diagram is done, except in small neighborhoods of the bifurcations. The proposed method, even though influenced by the work of van den Berg et al. [Math. Comp., **79**, 1565–1584 (2010)], introduces new analytic estimates, a new *gluing-free* approach for the construction of global smooth branches and provides a detailed analysis of the choice of the parameters to be made in order to maximize the chances of performing successfully the computational proofs.

Keywords

Equilibria of systems of PDEs · Bifurcation diagram · Contraction mapping · Rigorous numerics

Mathematics Subject Classification (2010): 65N15 · 37M20 · 35K55

1 Introduction

Establishing the existence of non constant bounded solutions to parameter dependent systems of reaction-diffusion PDEs is a classical problem in nonlinear analysis. Methods like singular perturbation theory [1], local bifurcation theory (see [2] and the references therein), the local theory of Crandall and Rabinowitz [3], and the Leray-Schauder degree theory can be used to prove existence of such non constant solutions. However, it appears difficult in practice to use such results to answer specific questions about the solutions, e.g. determining the number of (or a lower bound on the number of) non constant co-existing steady states. If the parameter dependent system under study undergoes a bifurcation from a trivial solution, it also appears difficult to determine rigorously the behaviour of the solutions on the global bifurcating branches. The global bifurcation theorem of Rabinowitz [4], although powerful and general, can convey only partial information about the global behaviour of the branches.

While the development of theoretical knowledge about existence of solutions of systems of PDEs is slow, meticulous and often hard to grasp for non experts, there exist several user friendly bifurcation softwares that can efficiently produce tremendous amount of bounded approximate solutions. However, with any numerical methods, there is the question of validity of the outputs.

The goal of this paper is to propose, in the context of studying non constant steady states for systems of PDEs, a rigorous computational method in an attempt to fill the gap between

*CMLA, ENS Cachan, 61 av. du Président Wilson, 94235 Cachan, France (mbreden@ens-cachan.fr).

†Département de Mathématiques et de Statistique, Université Laval, 1045 avenue de la Médecine, Québec, QC, G1V0A6, Canada (jean-philippe.lessard@mat.ulaval.ca). This author was supported by NSERC.

‡CMLA, ENS Cachan, 61 av. du Président Wilson, 94235 Cachan, France (mvanicat@ens-cachan.fr).

the above mentioned theoretical and computational advances. More specifically, we compute rigorously a global bifurcation diagram of steady states for the 3-component reaction-diffusion system arising in population dynamics introduced in [5], and given by

$$\begin{cases} \partial_t x = d\Delta x + (r_1 - a_1(x+y) - b_1 z)x + \dfrac{1}{\varepsilon}\left(y\left(1-\dfrac{z}{N}\right) - x\dfrac{z}{N}\right), \\ \partial_t y = (d+\beta N)\Delta y + (r_1 - a_1(x+y) - b_1 z)y - \dfrac{1}{\varepsilon}\left(y\left(1-\dfrac{z}{N}\right) - x\dfrac{z}{N}\right), \\ \partial_t z = d\Delta z + (r_2 - b_2(x+y) - a_2 z)z, \end{cases} \tag{1}$$

where $x = x(\xi,t)$, $y = y(\xi,t)$ and $z = z(\xi,t)$ are defined for $t > 0$, $\xi \in [0,1]$ with Neumann boundary conditions and with the following fixed numerical values $a_1 = 3$, $a_2 = 3$, $b_1 = 1$, $b_2 = 1$, $r_1 = 5$, $r_2 = 2$, $\beta = 3$, $\varepsilon = 0.01$ and $N = 1$. We consider the diffusion d as a free parameter. The above choice of fixed parameter values is chosen so that, when the parameter d varies, Turing's instability (e.g. [6]) can be observed. More precisely, varying the diffusion d can destabilize the constant steady state solution given by $(x,y,z) = (\frac{91}{64}, \frac{13}{64}, \frac{1}{8})$, which is stable for the corresponding finite dimensional ODE model without diffusion terms. Hence, by changing the diffusion d, interesting non trivial bounded stationary patterns can arise as a result of Turing's instability, which is one of the most important mechanisms of pattern formation. Note that considering a 3-component reaction-diffusion system allows having Turing instability with quadratic reaction terms, as opposed to the standard cubic case. A nice consequence of this choice of system is that the nonlinear terms are easier to estimate than in the cubic case.

The system of PDEs (1) has been introduced in [5] with the goal of studying the (theoretically harder to study) cross-diffusion model for the competitive interaction between two species

$$\begin{cases} \partial_t u_1(\xi,t) = \Delta[(d_1 + \alpha u_2)u_1] + (r_1 - a_1 u_1 - b_1 u_2)u_1, \\ \partial_t u_2(\xi,t) = \Delta[(d_2 + \beta u_1)u_2] + (r_2 - b_2 u_1 - a_2 u_2)u_2, \end{cases} \tag{2}$$

where $u_1 = u_1(\xi,t), u_2 = u_2(\xi,t)$ are defined for $t > 0$, $\xi \in [0,1]$, and satisfy Neumann boundary conditions. As already mentioned in [5], model (2) falls into quasi-linear parabolic systems so that even the existence problem of solutions is not trivial and has been investigated by several authors (e.g. see [7, 8, 9] and the references therein). It is shown in [5] that the solutions of (2) can be approximated by those of (1) in a finite time interval if the solutions are bounded and provided ε is small enough. It is also proved in [10] that the steady states of the reaction-diffusion system (1) approximates the steady states of the cross-diffusion system (2) as ε goes to 0. Hence, developing a rigorous computational approach to prove existence of non constant steady states of (1) seems to be an interesting problem, as it may shed some light on how to rigorously study non constant steady states of a cross-diffusion model (see Theorem 2). Here is a first result, whose proof can be found in Section 5.

Theorem 1 (Rigorous computation of a global bifurcation diagram). *Except in small neighborhoods of the bifurcations, each point in Figure 1 represents exactly one steady state for* (1)*, each curve on the diagram is smooth and between the apparent bifurcations (in black dots), there are no secondary bifurcations of steady states.*

Let us briefly introduce the ideas behind the rigorous method. First, the steady states (x,y,z) defined on $[0,1]$ of (1) with Neumann boundary conditions can be extended periodically on $[-1,1]$ and then expanded as Fourier series of the form $x(\xi) = \frac{x_0}{2} + \sum_{k\geq 1} x_k \cos(k\pi\xi)$, $y(\xi) = \frac{y_0}{2} + \sum_{k\geq 1} y_k \cos(k\pi\xi)$ and $z(\xi) = \frac{z_0}{2} + \sum_{k\geq 1} z_k \cos(k\pi\xi)$. Plugging the expansions of x, y and z in (1) and computing the Fourier coefficients of the resulting expansions yield the following infinite set of algebraic equations to be satisfied

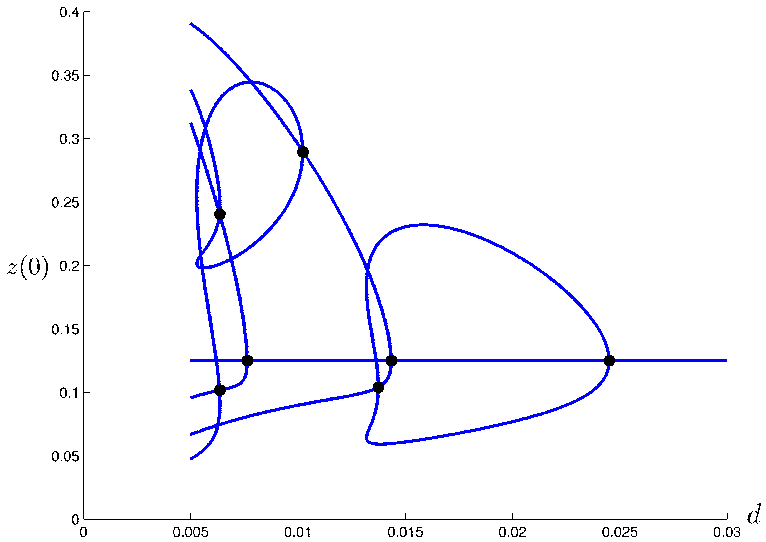

Figure 1: The rigorously computed bifurcation diagram of Theorem 1. Note that the apparent bifurcations which appear in black are not proved rigorously. The horizontal axis represents the diffusion parameter d while the vertical axis represents the value $z(0)$ of the steady state (x, y, z) of (1). The apparent intersections which are not denoted by black dots are not bifurcation points, e.g. see Figure 9 (c),(d) for a geometrical interpretation of apparently close solutions.

$$
\begin{aligned}
f_{n_x}(U) &\stackrel{\text{def}}{=} (r_1 - d(\pi n)^2)x_n + \frac{1}{\varepsilon}y_n - a_1[x^2]_n - a_1[x*y]_n - (b_1 + \frac{1}{\varepsilon N})[x*z]_n - \frac{1}{\varepsilon N}[y*z]_n = 0,\\
f_{n_y}(U) &\stackrel{\text{def}}{=} ((r_1 - \frac{1}{\varepsilon} - (d+\beta N)(\pi n)^2)y_n - a_1[y^2]_n - a_1[x*y]_n - (b_1 - \frac{1}{\varepsilon N})[y*z]_n + \frac{1}{\varepsilon N}[x*z]_n = 0,\\
f_{n_z}(U) &\stackrel{\text{def}}{=} (r_2 - d(\pi n)^2)z_n - a_2[z^2]_n - b_2[x*z]_n - b_2[y*z]_n = 0,
\end{aligned}
\tag{3}
$$

where $n \geq 0$, $[\phi * \varphi]_n \stackrel{\text{def}}{=} \frac{1}{2}\sum_{k\in\mathbb{Z}} \phi_{|k|}\varphi_{|n-k|}$ and where $\phi^2 = \phi * \phi$. Given $n \geq 0$, let $u_n \stackrel{\text{def}}{=} (x_n, y_n, z_n)$ the n-th Fourier coefficients of (x, y, z) and let $u \stackrel{\text{def}}{=} (u_n)_{n\geq 0}$. Define $U = (d, u)$ and let $f_n(U) \stackrel{\text{def}}{=} (f_{n_x}(U), f_{n_y}(U), f_{n_z}(U))$, where each component is defined by (3). Finally define $f(U) = (f_n(U))_{n\geq 0}$. In order to compute steady states of (1), we will be looking for solutions U of $f(U) = 0$ in a Banach space of fast decaying coefficients. Let us be more explicit about this. As in [11], we define weight functions ($q > 1$)

$$
\omega_n^q = \begin{cases} 1, & n = 0; \\ n^q, & n \geq 1, \end{cases} \tag{4}
$$

which are used to define, for $u = (u_n)_{n\geq 0}$ as defined above, the norm

$$
\|u\|_q = \sup_{n\in\mathbb{N}} |u_n|_\infty \, \omega_n^q, \tag{5}
$$

where $q > 1$ is a decay rate and $|u_n|_\infty = \max(|x_n|, |y_n|, |z_n|)$. Define

$$
\|U\|_q = \max\left\{ \frac{|d|}{\rho}, \|u\|_q \right\} \tag{6}
$$

where ρ is a constant whose value will be chosen later, and $\Omega_q = \left\{ U = (d, u) \mid \|U\|_q < \infty \right\}$, a Banach space with norm (6) of sequences decreasing to zero at least as fast as n^{-q}, as $n \to \infty$.

Lemma 1. *Fix a diffusion parameter d and a decay rate $q > 1$. Using the above construction, $U = (d, u) \in \Omega_q$ is a solution of $f(U) = 0$ if and only if (x, y, z) is a strong C^2-solution of the stationary Neumann problem of* (1).

Proof. Assume that $U = (d, u) \in \Omega_q$ is a solution of $f(U) = 0$. Since Ω_q is a Banach algebra for $q > 1$ (see Section 3.5), then one can use a bootstrap argument (e.g. like the one in Section 3.3) with the fact that $\Omega_q \subset \Omega_{q_0}$ for any $q_0 \in (1, q]$ to get that $U \in \Omega_{q_0}$, for every $q_0 > 1$. By construction of f given component-wise by (3), (x, y, z) defined by the Fourier coefficients $(u_n)_{n\geq 0} = (x_n, y_n, z_n)_{n\geq 0}$ is then a strong C^2-solution of the stationary Neumann problem of (1). Now, if (x, y, z) is a strong C^2-solution of the stationary Neumann problem of (1), it is in fact, by a bootstrap argument on the PDE, a C^∞-solution. Hence, the Fourier coefficients of (x, y, z) decrease faster than any algebraic decay, which implies that $U \in \Omega_q$, for all $q > 1$. □

Hence, based on the result of Lemma 1, we focus our attention on finding $U \in \Omega_q$ such that $f(U) = 0$, for a fixed $q > 1$. To find the zeros of f, the idea is the following. Find an approximate solution $\overline{U} \in \Omega_q$ of $f = 0$, which is done by applying Newton's method on a finite dimensional projection of f. Then construct a nonlinear operator $T : \Omega_q \to \Omega_q$ satisfying two properties. First, it is defined so that the zeros of f are in one-to-one correspondence with the fixed points of T, that is $f(U) = 0$ if and only if $T(U) = U$. Second, it is constructed as a Newton-like operator around the numerical approximation $\overline{U}$. The final and most involved step is to look for the existence of a set $B \subset \Omega_q$ centered at $\overline{U}$ which contains a genuine zero of the nonlinear operator f. The idea to perform such task is to find $B \subset \Omega_q$ such that $T : B \to B$ is a contraction, and to use the contraction mapping theorem to conclude about the existence of a unique fixed point of T within B. The method used to find B is based on the notion of the radii polynomials, which provide an efficient means of finding a set on which the contraction mapping can be applied [12]. We refer to Section 2.2 for the definition of the radii polynomials and to Section 3.8 for their explicit construction. The polynomials are used to find (if possible) an $r > 0$ such that T is a contraction on the closed ball $B(\overline{U}, r)$ of radius r and centered at $\overline{U}$ in Ω_q, for $\|\cdot\|_q$. With this norm, the closed ball is given by

$$B(U, r) = U + \left[-\frac{r}{\rho}, \frac{r}{\rho}\right] \times \prod_{n\in\mathbb{N}} \left[-\frac{r}{\omega_n^q}, \frac{r}{\omega_n^q}\right]^3. \tag{7}$$

The above scheme to enclose uniquely and locally zeros of f can be extended to find smooth solution paths $\{\tilde{U}(s)\}_{s\in I}$ such that $f(\tilde{U}(s)) = 0$ for all $s \in I$ in some interval I. The idea is to construct radii polynomials defined in terms of both r and s and to apply the uniform contraction principle. With this construction, it is possible to prove existence of smooth global solution curves of $f = 0$. See Section 2.2 for more details.

Before proceeding further, it is worth mentioning that the method proposed in the present work is strongly influenced by the method based on the radii polynomials introduced in [12] and the rigorous branch following method of [11]. There are however some differences. First, prior to the present work, the method based on the radii polynomials has never been applied to systems of reaction-diffusion PDEs. Second, new convolution estimates are introduced in Section 3.5 for a new range of decay rates, that is for $q \in (1, 2)$. The importance of these new estimates is that they can improve the success rate of the proofs while reduce significantly the computational time. Indeed, it is demonstrated in Section 4.2 that using $q < 2$ can greatly improve the efficiency of the rigorous method based on the radii polynomials. Also in Section 4.2, a detailed analysis of the optimal choice of the decay rate parameter $q > 1$ is made, where the goal is to maximize the chances of performing successfully the computational proofs. Note that prior to the present work, the method based on the radii polynomials has only used decay rates $q \geq 2$. Third, the method here is slightly different from the approach of [11] for the construction of global branches in the sense that it is a *gluing-free* approach. More precisely, it means that no extra work has to be made to glue together adjacent small pieces of smooth curves (see Theorem 6). This is due to the fact that here, a global C^0 piecewise linear numerical approximation of the curve is constructed, while in [11], the global representation of the curve is piecewise linear but not C^0.

Let us present a consequence of Theorem 1. This result could be hard to prove with a purely analytic approach. Its proof is presented in Section 5 and see Figure 2 for a representation.

Corollary 1 (**Co-existence of non constant steady states).** *Consider 3-component reaction-diffusion system of PDEs* (1) *with the fixed diffusion parameter* $d = 0.006$. *Then* (1) *has at least eleven distinct co-existing steady states with ten of them being non constant.*

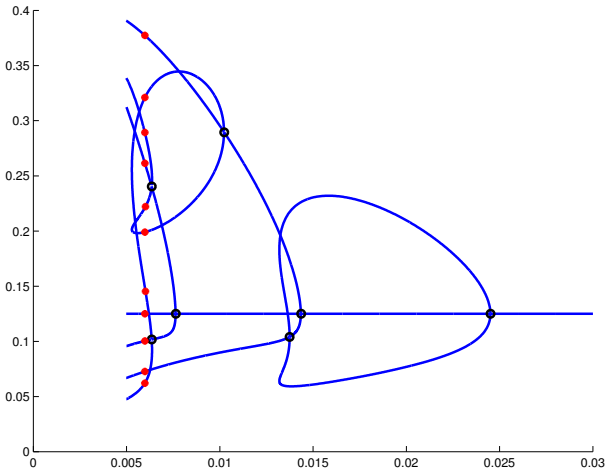

Figure 2: Geometrical interpretation of Corollary 1. In red, eleven co-existing steady states of (1) at the parameter value $d = 0.006$. Ten of these solutions are non constant.

The following result may be a step toward rigorously studying steady states of the cross-diffusion model (2). Its proof is omitted since similar to the proof of Theorem 1.

Theorem 2 (**Rigorous computations of approximations for a cross-diffusion model).** *Fix* $d = 0.02$. *For each* $\varepsilon \in \{10^{-2}, 10^{-3}, 10^{-4}, 10^{-5}\}$, *there exist a non-trivial steady state solution* $(x_\varepsilon, y_\varepsilon, z_\varepsilon)$ *of the reaction-diffusion system* (1). *See Figure 3 for a representation.*

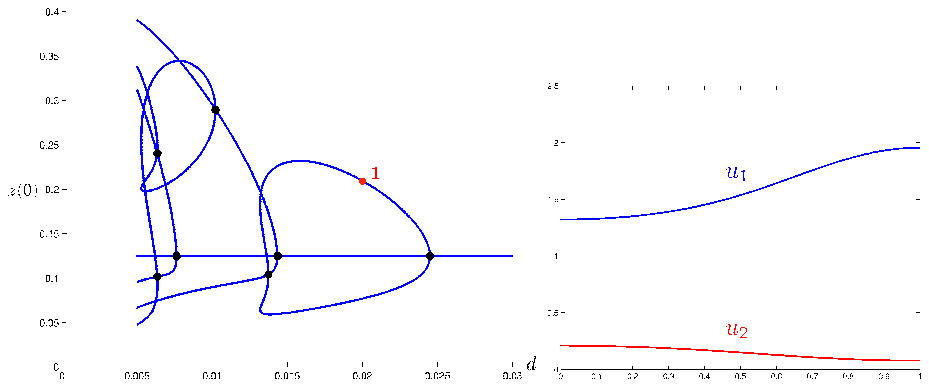

(a) Diagram of Theorem 1 with point **1** (in red) corresponding to the starting point of the continuation done in the proof of Theorem 2 as $\varepsilon \searrow 0$.

(b) (u_1, u_2) at $\varepsilon = 10^{-2}$ corresponding to the red point on the bifurcation diagram on the left.

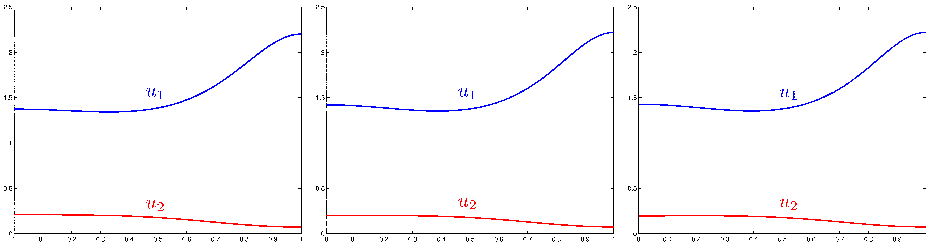

(c) (u_1, u_2) at $\varepsilon = 10^{-3}$

(d) (u_1, u_2) at $\varepsilon = 10^{-4}$

(e) (u_1, u_2) at $\varepsilon = 10^{-5}$

Figure 3: Corresponding to the rigorously computed steady states $(x_\varepsilon, y_\varepsilon, z_\varepsilon)$ of (1) from Theorem 2, we define $u_1(\varepsilon) = x_\varepsilon + y_\varepsilon$ and $u_2(\varepsilon) = z_\varepsilon$. There is apparent convergence as ε approaches zero.

The solutions in Figure 3 are rigorously computed using the method presented in this paper. In fact the computation uses a simpler version of the method because the proofs of existence are only done at discrete values of the parameters. As can be seen in Table 1, there is apparent convergence as ε goes to zero. The $\|\cdot\|_\infty$ bounds there are rigorous because we control through $r = 10^{-8}$ (the radius of the ball (7)) the error we have made with the numerical approximations. According to the work of [10], the solution on Figure 3(e) given by $(u_1(\varepsilon), u_2(\varepsilon)) = (x_\varepsilon + y_\varepsilon, z_\varepsilon)$ when $\varepsilon = 10^{-5}$ should be close to a solution of the cross-diffusion system (2).

ε_1	ε_2	$\max\left(\|u_1(\varepsilon_1) - u_1(\varepsilon_2)\|_\infty, \|u_2(\varepsilon_1) - u_2(\varepsilon_2)\|_\infty\right)$
10^{-2}	10^{-3}	0.2918
10^{-3}	10^{-4}	0.0757
10^{-4}	10^{-5}	0.0092

Table 1: Apparent convergence of the rigorously computed steady states of the 3-component reaction-diffusion system (1) toward a steady state of the cross-diffusion system (2).

The paper is organized as follows. In Section 2, the general method is introduced. In Section 3, the method is applied to the problem of computing rigorously steady states of the 3-component reaction-diffusion system (1), where the radii polynomials are explicitly constructed in this context. In Section 4, a detailed analysis of the optimal choice of the parameters Δ_s, m and q is made, with the goal of maximizing the chances of performing successfully the computational proofs. Finally, in Section 5, the proofs of Theorem 1 and Corollary 1 are presented.

2 Description of the general method

In this section, we present the general method, leaving some technical details to Section 3, where all the computations and estimates are presented explicitly to compute several global smooth branches of steady states of (1). The attention is now focused on describing a general method to prove existence and compute global smooth solution curves of $f(U) = 0$ in a Banach space Ω_q of fast decaying Fourier coefficients. The method is based on the radii polynomials, first introduced in [12], and is strongly influenced by the rigorous branch following method of [11]. The idea is to compute a set of numerical approximations $\{\overline{U}_0, \ldots, \overline{U}_j\}$ of $f = 0$ by considering a finite dimensional projection, to use the approximations to construct a global continuous curve of piecewise linear interpolations between the $\overline{U}_i$'s (see Figure 5) and to apply the uniform contraction principle on *tubes* centered at each segment to conclude about the existence of a unique smooth solution curve of $f = 0$ nearby the piecewise linear curve of approximations. The approximate curve is computed using pseudo-arclength continuation (e.g. [13]).

2.1 Construction of a piecewise linear curve of approximations

To construct a piecewise linear curve of approximations of $f = 0$, we consider a finite dimensional projection $f^{[m]}$ of f whose dimension depends on m (see Section 3.1). In what follows, $(\cdot)^{[m]}$ denotes considering this finite dimensional projection. Reversely, when we have some finite dimensional vector $U^{[m]}$, U denotes the infinite vector obtained by completing $U^{[m]}$ with zeros.

Suppose we have an approximate zero $\overline{u}_0^{[m]}$ of $f^{[m]}(d_0, \cdot)$ at d_0. Then, given $U_0^{[m]} \overset{\text{def}}{=} \left(d_0, u_0^{[m]}\right)$, we compute an approximate tangent vector $\dot{U}_0^{[m]}$, that is $Df^{[m]}\left(\overline{U}_0^{[m]}\right)\left(\dot{U}_0^{[m]}\right) \approx 0$. Consider

$$\hat{U}_0^{[m]} \overset{\text{def}}{=} \overline{U}_0^{[m]} + \Delta_s \dot{U}_0^{[m]}, \tag{8}$$

a predictor, where Δ_s is a parameter (whose value, representing roughly the arc length of curve we are covering in one step, is discussed in Section 4.1). Consider also the plane Π whose equation is given by $E(U) \overset{\text{def}}{=} \left(U - \hat{U}_0\right) \cdot \dot{U}_0 = 0$. The pseudo-arclength operator is

$$F : U \mapsto \begin{pmatrix} E(U) \\ f(U) \end{pmatrix},$$

and using Newton's method with initial point $\hat{U}_0^{[m]}$, we compute $U_1^{[m]}$ such that $F^{[m]}(U_1^{[m]}) \approx 0$. We refer to Figure 4 for a geometrical representation of a pseudo-arclength continuation step. A next predictor-corrector step can be performed starting at $U_1^{[m]}$, and so on.

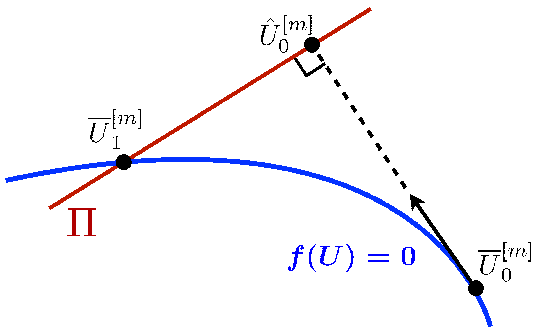

Figure 4: A predictor-corrector step with pseudo-arclength continuation.

Applying the predictor-corrector step j times, we compute a set $\{\overline{U}_0, \ldots, \overline{U}_j\}$ of approximations that defines a piecewise linear approximation curve (see Figure 5). The next step is to

show existence of a unique smooth solution curve $\mathcal{C}$ of $f = 0$ nearby the piecewise linear curve of approximations, as portrayed in Figure 5. This task is twofold. First, one shows the existence of a unique portion of solution curve $\mathcal{C}^{(i)}$ in a small tube centered at the segment $[\overline{U}_i, \overline{U}_{i+1}]$. This is done in Theorem 3 by showing that a Newton-like operator $\tilde{T}$ is a uniform contraction on the tube. To verify the hypothesis of the uniform contraction principle, Theorem 4 is introduced. This requires the construction of some bounds, which are presented in Section 2.2.1. In practice, verifying the hypothesis of Theorem 4 is done via Lemma 2 by using the radii polynomials which are presented in Section 2.2.2. From Lemma 2, one sees that the strength of the radii polynomials is that they provide an efficient means (in the form of a finite number of polynomial inequalities to be checked rigorously on a computer using interval arithmetic) of finding a set on which $\tilde{T}$ is a uniform contraction. Second, one shows that each $\mathcal{C}^{(i)}$ is smooth, and that

$$\mathcal{C} \overset{\text{def}}{=} \bigcup_{i=0}^{j-1} \mathcal{C}^{(i)}$$

is a global smooth solution curve of $f = 0$. In Section 2.3, we show how the smoothness of $\mathcal{C}^{(i)}$ can be proved by verifying the hypothesis of Theorem 5. Afterward, we show that if the hypotheses of Theorem 5 and Theorem 6 are satisfied, then $\mathcal{C}^{(i)}$ and $\mathcal{C}^{(i+1)}$ connect smoothly. The smoothness of the global solution curve $\mathcal{C}$ follows by construction.

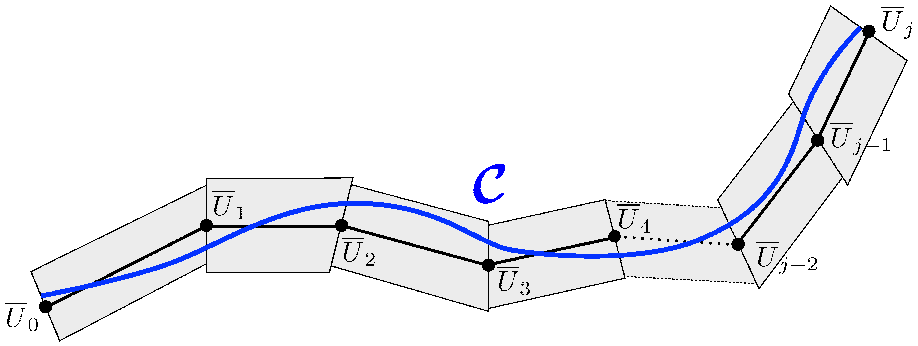

Figure 5: Piecewise linear curve approximation (in black) constructed using pseudo-arclength continuation and existence of a global smooth solution curve $\mathcal{C}$ of $f = 0$ (in blue) nearby the approximations

2.2 Newton-like operator, uniform contraction and radii polynomials

Let us define what is required to prove existence of some portion of smooth curve $\mathcal{C}^{(i)}$. Without loss of generality, let us introduce the idea to prove the existence of $\mathcal{C}^{(0)}$ that is the piece of curve close to the segment $[\overline{U}_0, \overline{U}_1]$ with two approximate tangent vectors $\dot{U}_0$ and $\dot{U}_1$ at those points given by the pseudo-arclength continuation algorithm. For any s in $[0, 1]$, we set

$$\overline{U}_s \overset{\text{def}}{=} (1-s)\overline{U}_0 + s\overline{U}_1 = \overline{U}_0 + s\Delta\overline{U}, \text{ where } \Delta\overline{U} \overset{\text{def}}{=} \overline{U}_1 - \overline{U}_0$$

and

$$\dot{U}_s \overset{\text{def}}{=} (1-s)\dot{U}_0 + s\dot{U}_1 = \dot{U}_0 + s\Delta\dot{U}, \text{ where } \Delta\dot{U} \overset{\text{def}}{=} \dot{U}_1 - \dot{U}_0.$$

Then we define, still for s in $[0, 1]$, the hyperplane Π_s whose equation is given by

$$E_s(U) \overset{\text{def}}{=} \left(U - \overline{U}_s\right) \cdot \dot{U}_s, \tag{9}$$

the function

$$F_s(U) \overset{\text{def}}{=} \begin{pmatrix} E_s(U) \\ f(U) \end{pmatrix} \tag{10}$$

and the Newton-like operator

$$T_s(U) \stackrel{\text{def}}{=} U - JF_s(U), \tag{11}$$

where J is an injective linear operator approximating the inverse of $DF_0\left(\overline{U}_0\right)$ (see Section 3.2 for an example of how to construct J and check that it is injective). We now use the uniform contraction principle on T_s to conclude about the existence of a curve of fixed points that corresponds, by injectivity of J, to a solution curve of $f(U) = 0$.

Theorem 3. *If there exists some $r > 0$ such that*

$$\tilde{T} : \begin{cases} [0,1] \times B(0,r) \longrightarrow B(0,r) \\ (s,V) \longmapsto T_s\left(V + \overline{U}_s\right) - \overline{U}_s \end{cases}$$

is a uniform contraction, then for every $s \in [0,1]$, there exists a unique $\tilde{U}(s) \in B\left(\overline{U}_s, r\right)$ such that $F_s\left(\tilde{U}(s)\right) = 0$. Moreover, the function $s \mapsto \tilde{U}(s)$ is of class C^k if $(s,V) \mapsto \tilde{T}(s,V)$ is of class C^k.

Proof. This is a direct application of the uniform contraction principle (e.g. see [14]). □

It seems legitimate to expect T_s to be a contraction on a small set containing the segment $[\overline{U}_0, \overline{U}_1]$ parameterized by $\overline{U}_s$ ($s \in [0,1]$) since T_s is an approximate Newton operator at $\overline{U}_0$.

2.2.1 Definition of some bounds

To prove that $\tilde{T}$ is a uniform contraction on $B(0,r)$, we prove the existence of bounds $Y_d(s)$, $Y_n(s)$, $Z_d(r,s)$ and $Z_n(r,s)$ such that for every $n \in \mathbb{N}$ and $s \in [0,1]$,

$$\left|\left[T_s\left(\overline{U}_s\right) - \overline{U}_s\right]_d\right| \leq Y_d(s) \text{ and } \left|\left[T_s\left(\overline{U}_s\right) - \overline{U}_s\right]_n\right| \leq Y_n(s), \tag{12}$$

$$\sup_{V,V' \in B(0,r)} \left|\left[DT_s\left(\overline{U}_s + V\right)\left(V'\right)\right]_d\right| \leq Z_d(r,s) \text{ and } \sup_{V,V' \in B(0,r)} \left|\left[DT_s\left(\overline{U}_s + V\right)\left(V'\right)\right]_n\right| \leq Z_n(r,s). \tag{13}$$

The subscript $(\cdot)_d$ corresponds to the first entry d of U and the first entry E_s of F_s. We set $Y = (Y_d, Y_0, \ldots, Y_n, \ldots)$, where $Y_n \in \mathbb{R}^3$ (same for Z). Absolute values and inequalities applied to vectors are considered component-wise. For the sake of simplicity of the presentation, we omit to write explicitly the dependence of those terms in r and s when we are not focusing on them. Let us now give some sufficient conditions on those bounds for $\tilde{T}$ to be a uniform contraction.

Theorem 4. *If Y, Z verify (12) and (13) resp, and if there exists $r > 0$ such that for all $s \in [0,1]$*

$$\|Y(s) + Z(r,s)\|_q < r, \tag{14}$$

then $\tilde{T}$ is a uniform contraction on $B(0,r)$, with contraction constant $\kappa \stackrel{\text{def}}{=} \max_{s \in [0,1]} \dfrac{\|Z(r,s)\|_q}{r} < 1$.

Proof. For all $s \in [0,1]$, $j \in \cup_{n \geq 0}\{n_x, n_y, n_z\}$, $V, V' \in B\left(\overline{U}_s, r\right)$, the mean value theorem yields the existence of $W = \lambda V + (1-\lambda)V'$ for some $\lambda = \lambda(j) \in [0,1]$, such that

$$\left[T_s(V) - T_s(V')\right]_j = \left[DT_s(W)(V - V')\right]_j.$$

Then

$$\left|\left[T_s(V) - T_s(V')\right]_j\right| \leq \left|\left[DT_s(W)\left(\frac{r(V-V')}{\|V-V'\|_q}\right)\right]_j\right| \frac{1}{r}\|V - V'\|_q \leq \frac{Z_j(r,s)}{r}\|V - V'\|_q.$$

Similarly,

$$\left|\left[T_s(V) - T_s(V')\right]_d\right| \leq \frac{Z_d(r,s)}{r} \left\|V - V'\right\|_q.$$

Therefore, for all $s \in [0,1]$ and $V, V' \in B(0,r)$,

$$\left\|\tilde{T}(s,V) - \tilde{T}(s,V')\right\|_q = \left\|T_s\left(V + \overline{U}_s\right) - T_s\left(V' + \overline{U}_s\right)\right\|_q \leq \frac{\|Z(r,s)\|_q}{r} \left\|V - V'\right\|_q = \kappa \left\|V - V'\right\|_q$$

and for all $s \in [0,1]$ and $V \in B(0,r)$,

$$\left\|\tilde{T}(s,V)\right\|_q = \left\|T_s(V) - \overline{U}_s\right\|_q \leq \left\|T_s(V) - T_s\left(\overline{U}_s\right)\right\|_q + \left\|T_s\left(\overline{U}_s\right) - \overline{U}_s\right\|_q \leq \|Z(r,s) + Y(s)\|_q < r.$$

□

Suppose the bounds Y and Z verifying conditions (12) and (13) are computed. To be able to use Theorem 4, we need to check that those bounds also verify inequality (14). Note that for every $n \in \mathbb{N}$, Y_n is a function of s and Z_n is a function of both r and s. Besides, they can be constructed as polynomials in r and s, and for n greater than some M, we can choose

$$Y_n = 0 \quad \text{and} \quad Z_n = \hat{Z}_M \frac{\omega_M^q}{\omega_n^q},$$

where $\hat{Z}_M$ is also a polynomial in r and s. Those assertions are not explained in details here. We refer to Section 3.6.2 and Section 3.7.3 for explicit details. For the moment, let us only say that Y_n can be taken to be 0 for n large enough because $\overline{U}_s$ has only a finite number m of non zero coefficients, and hence $\left[T_s\left(\overline{U}_s\right) - \overline{U}_s\right]_n = 0$ for n large enough. Let us now introduce the radii polynomials which allow us to verify inequality (14) using rigorous numerics.

2.2.2 Radii polynomials

Let M be a computational parameter. We refer to Section 3.6 to determine how to choose its value. Define

$$P_d(r,s) \overset{\text{def}}{=} Y_d(s) + Z_d(r,s) - \frac{r}{\rho},$$

for $0 \leq n < M$,

$$P_n(r,s) \overset{\text{def}}{=} Y_n(s) + Z_n(r,s) - \frac{r}{\omega_n^q},$$

and for $n = M$,

$$P_M(r,s) \overset{\text{def}}{=} \hat{Z}_M(r,s) - \frac{r}{\omega_M^q}.$$

Note that the term $-\frac{r}{\omega_n^q}$ has to be understood component-wise.

Lemma 2. *Suppose that there exists $r > 0$ such that for all $s \in [0,1]$,*

$$P_d(r,s) < 0 \quad \textit{and} \quad P_n(r,s) < 0 \quad \text{for all } 0 \leq n \leq M.$$

Then inequality (14) *is satisfied and Theorem 4 holds.*

Proof. By definition of the radii polynomials, we have that

$$Y_d(s) + Z_d(r,s) < \frac{r}{\rho} \qquad \text{and} \qquad Y_n(s) + Z_n(r,s) < \frac{r}{\omega_n^q}$$

for all $0 \leq n \leq M$. Since $P_M(r,s) = \hat{Z}_M(r,s) - \frac{r}{\omega_M^q} < 0$, we also have that

$$Y_n(s) + Z_n(r,s) = \hat{Z}_M(r,s)\frac{\omega_M^q}{\omega_n^q} < \frac{r}{\omega_n^q},$$

for all $n > M$. Therefore inequality (14) is satisfied. □

We show in Section 4.1 how to carefully chose Δ_s and m to maximize the chance of finding an $r > 0$ satisfying the hypotheses of Lemma 2. Lemma 2 is useful for checking efficiently the hypotheses of Theorem 4, and therefore Theorem 3 by verifying a finite number of inequalities.

2.3 Constructing a global smooth solution curve

Suppose now that we found $r > 0$ satisfying the radii polynomials inequalities of Lemma 2. Hence, by Theorem 3, there exists a smooth function $s \in [0,1] \mapsto \tilde{U}(s)$ whose image $\mathcal{C}^{(0)}$ is the only solution curve to $f = 0$ within in a small tube of radius r centered at the segment $[\overline{U}_0, \overline{U}_1]$. More precisely, this tube is given by $\left\{U \mid \exists s \in [0,1],\ U \in B\left(\overline{U}_s, r\right) \cap \Pi_s\right\}$. The following result is similar to Lemma 10 in [11].

Theorem 5. *Suppose that*

$$-\Delta\overline{U} \cdot \dot{U}_0 + r\,(W_1^q)^{[m]} \cdot \left|\Delta\dot{U}\right| + \left|\Delta\overline{U} \cdot \Delta\dot{U}\right| < 0, \tag{15}$$

where

$$(W_1^q)^{[m]} = \left(\frac{1}{\rho}, \underbrace{\frac{1}{\omega_0^q}, \ldots, \frac{1}{\omega_0^q}}_{3\ \ times}, \ldots, \underbrace{\frac{1}{\omega_{m-1}^q}, \ldots, \frac{1}{\omega_{m-1}^q}}_{3\ \ times}\right)^T,$$

then $\mathcal{C}^{(0)}$ is a smooth curve, that is, for all $s \in [0,1]$, $\dfrac{d\tilde{U}}{ds}(s) \neq 0$.

Proof. Considering the equality $E_s(\tilde{U}(s)) = 0$ and taking its derivative with respect to s,

$$\frac{d\tilde{U}}{ds}(s) \cdot \dot{U}_s = -\frac{\partial E_s}{\partial s}(\tilde{U}(s)).$$

Recalling the definition of E_s from (9),

$$\frac{\partial E_s}{\partial s}(\tilde{U}(s)) = -\Delta\overline{U} \cdot \dot{U}_0 + \left(\tilde{U}(s) - \overline{U}_s\right) \cdot \Delta\dot{U} - s\Delta\overline{U} \cdot \Delta\dot{U}. \tag{16}$$

Hence, for all $s \in [0,1]$,

$$\frac{\partial E_s}{\partial s}(\tilde{U}(s)) \leq -\Delta\overline{U} \cdot \dot{U}_0 + r\,(W_1^q)^{[m]} \cdot \left|\Delta\dot{U}\right| + s\left|\Delta\overline{U} \cdot \Delta\dot{U}\right|,$$

since $\left\|\tilde{U}(s) - \overline{U}_s\right\|_q < r$. Finally, using inequality (15), for all $s \in [0,1]$, $\dfrac{\partial E_s}{\partial s}(\tilde{U}(s)) \neq 0$. This proves that for all $s \in [0,1]$, $\dfrac{d\tilde{U}}{ds}(s) \neq 0$, yielding the smoothness of $\mathcal{C}^{(0)}$. □

In practice, the hypothesis of Theorem 5 are checked rigorously using interval arithmetic. Remark that this hypothesis is very reasonable if r is small enough. See Figure 6 for a geometric representation of the important quantities involved in the hypothesis (15). One can see there that if the length of the segment $[\overline{U}_0, \overline{U}_1]$ is small, that is if the vector $\Delta\overline{U}$ is small, then the vectors $\Delta\overline{U}$ and $\Delta\dot{U}$ should be close to be perpendicular and the vectors $\Delta\overline{U}$ and $\dot{U}_0$ should be close to be parallel. Hence, $\Delta\overline{U} \cdot \dot{U}_0$ should be close to the value $\|\Delta\overline{U}\|\|\dot{U}_0\|$ while the vector $\Delta\overline{U} \cdot \Delta\dot{U}$ should be close to 0. Hence, for very small value of r, the value of $r\,(W_1^q)^{[m]} \cdot \left|\Delta\dot{U}\right|$ should be small, and then the chances of satisfying inequality (15) should be high.

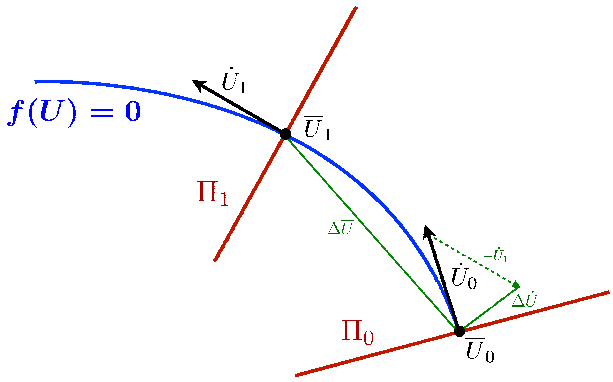

Figure 6: The important quantities involved in the hypothesis (15) of Theorem 5.

Assuming that two consecutive smooth curves have been computed, we can prove that they connect smoothly in one curve. Using the notation $(\cdot)^{(0)}$ (resp. $(\cdot)^{(1)}$) to refer to the first (resp. the second) portion of curve. The following result is similar to Proposition 8 in [11] but two aspects are different. First the gluing of $\mathcal{C}^{(0)}$ and $\mathcal{C}^{(1)}$ comes for free from the C^0 representation of the union of the segments $[\overline{U}_0, \overline{U}_1]$ and $[\overline{U}_1, \overline{U}_2]$. Second, the proof that $\mathcal{C}^{(0)} \cup \mathcal{C}^{(1)}$ is smooth at the intersection $\mathcal{C}^{(0)} \cap \mathcal{C}^{(1)}$ is more detailed and calls upon the implicit function theorem.

Theorem 6. *Assume that the hypotheses* (14) *of Theorem 4 and* (15) *of Theorem 5 are satisfied between* $\overline{U}_0$ *and* $\overline{U}_1$*, and also between* $\overline{U}_1$ *and* $\overline{U}_2$*. Then* $\mathcal{C}^{(0)} \cup \mathcal{C}^{(1)}$ *is a smooth curve.*

Proof. Since Theorem 4 is satisfied over the segment $[\overline{U}_0, \overline{U}_1]$ (resp. $[\overline{U}_1, \overline{U}_2]$), consider the radius $r^{(0)}$ (resp. $r^{(1)}$) satisfying (14). Without loss of generality, one can assume that $r^{(0)} \neq r^{(1)}$ by continuity of the radii polynomials. Theorem 4 allows us to use Theorem 3 to get the existence of two smooth functions $\tilde{U}^{(0)}$ and $\tilde{U}^{(1)}$ whose images are $\mathcal{C}^{(0)}$ and $\mathcal{C}^{(1)}$. First we prove that the two curves connect, that is $\tilde{U}^{(0)}(1) = \tilde{U}^{(1)}(0)$. Recalling (10), we have that $F_1^{(0)} = F_0^{(1)}$, in particular $\overline{U}_1^{(0)} = \overline{U}_1 = \overline{U}_0^{(1)}$ and $\Pi_1^{(0)} = \Pi_0^{(1)}$. Moreover, $\tilde{U}^{(0)}(1)$ is the only solution of $F_1^{(0)} = 0$ in $B\left(\overline{U}_1, r^{(0)}\right)$ and $\tilde{U}^{(1)}(0)$ is the only solution of $F_0^{(1)} = 0$ in $B\left(\overline{U}_1, r^{(1)}\right)$. Hence $\tilde{U}^{(0)}(1)$ and $\tilde{U}^{(1)}(0)$ are both solutions to $F_0^{(1)} = 0$ and since one of the two balls must be included into the other (they have same center) the two solutions are equal.

From now we assume without loss of generality that $r^{(0)} < r^{(1)}$ and we show that the connection between the two curves is smooth. For all s in $[0, 1]$, the radii polynomials are negative at $r^{(0)} > 0$. The fact that the radii polynomials are continuous in s yields the existence of $\varepsilon_0 > 0$ such that those polynomials are still negative for s in $[0, 1 + \varepsilon_0]$, and then that $\tilde{T}^{(0)}$ is still a uniform contraction for $[0, 1 + \varepsilon_0]$. As a result, $\tilde{U}^{(0)}$ can be extended into a smooth function defined on $[0, 1 + \varepsilon_0]$ such that $f\left(\tilde{U}^{(0)}(s)\right) = 0$, for all s in $[0, 1 + \varepsilon_0]$. Hence, $\tilde{U}^{(0)}\left([1, 1 + \varepsilon_0]\right) \subset \mathcal{C}^{(1)}$. We want to find $s \in [0, 1]$ such that $\tilde{U}^{(0)}(1 + \varepsilon) \in \Pi_s^{(1)}$ for all $\varepsilon \in [0, \varepsilon_0]$. To do that, set

$$\varphi : (\varepsilon, s) \longmapsto \left(\tilde{U}^{(0)}(1 + \varepsilon) - \overline{U}_s^{(1)}\right) \cdot \dot{U}_s^{(1)}.$$

We have $\varphi(0, 0) = \left(\tilde{U}^{(0)}(1) - \overline{U}_1\right) \cdot \dot{U}_1 = 0$ and $\varphi(0, s) = E_s^{(1)}\left(\tilde{U}^{(0)}(1)\right)$, so

$$\frac{\partial \varphi}{\partial s}(0, 0) = \left.\frac{\partial E_s^{(1)}}{\partial s}\right|_{s=0} \left(\tilde{U}^{(0)}(1)\right).$$

Since the hypothesis of Theorem 5 is verified, we get according to (16) that $\dfrac{\partial \varphi}{\partial s}(0, 0) < 0$. Hence the implicit function theorem holds and there exist $\varepsilon_1 \in (0, \varepsilon_0]$ and a smooth function $s : \varepsilon \in$

$[0,\varepsilon_1] \mapsto s(\varepsilon)$, such that $s(0)=0$ and $\varphi(\varepsilon, s(\varepsilon))=0$. Also,

$$\frac{\partial \varphi}{\partial \varepsilon}(0,0) + \frac{\partial \varphi}{\partial s}(0,0)s'(0) = 0,$$

and since

$$\frac{\partial \varphi}{\partial \varepsilon}(0,0) = \frac{d\tilde{U}}{ds}^{(0)}(1) \cdot \dot{U}_1 > 0 \text{ and } \frac{\partial \varphi}{\partial s}(0,0) < 0 \text{ according to (16) and the hypotheses,}$$

we have that $s'(0) > 0$. Hence, there exists $\varepsilon_2 \in (0,\varepsilon_1]$ such that for all $\varepsilon \in [0,\varepsilon_2]$, $s(\varepsilon) \in [0,1]$ and $F^{(1)}_{s(\varepsilon)}\left(\tilde{U}^{(0)}(1+\varepsilon)\right) = 0$. Given that for all $\varepsilon \in [0,\varepsilon_2]$, $F^{(1)}_{s(\varepsilon)} = 0$ has a unique solution in $B\left(\overline{U}^{(1)}_{s(\varepsilon)}, r^{(1)}\right)$, showing that $\left\|\tilde{U}^{(0)}(1+\varepsilon) - \overline{U}^{(1)}_{s(\varepsilon)}\right\|_q < r^{(1)}$ will conclude the proof. Now,

$$\begin{aligned}\left\|\tilde{U}^{(0)}(1+\varepsilon) - \overline{U}^{(1)}_{s(\varepsilon)}\right\|_q &\leq \left\|\tilde{U}^{(0)}(1+\varepsilon) - \overline{U}^{(0)}_{1+\varepsilon}\right\|_q + \left\|\overline{U}^{(0)}_{1+\varepsilon} - \overline{U}^{(0)}_1\right\|_q + \left\|\overline{U}^{(1)}_0 - \overline{U}^{(1)}_{s(\varepsilon)}\right\|_q \\ &\leq r^{(0)} + \varepsilon\left\|\Delta\overline{U}^{(0)}\right\|_q + s(\varepsilon)\left\|\Delta\overline{U}^{(1)}\right\|_q.\end{aligned}$$

Using that $s(0)=0$, that $s(\varepsilon)$ is continuous and that $r^{(0)} < r^{(1)}$, there exists $\varepsilon_3 \in [0,\varepsilon_2]$, such that for all $\varepsilon \in [0,\varepsilon_3]$,

$$\left\|\tilde{U}^{(0)}(1+\varepsilon) - \overline{U}^{(1)}_{s(\varepsilon)}\right\|_q < r^{(1)}.$$

By uniqueness, $\tilde{U}^{(0)}([1,1+\varepsilon_3]) \subset \mathcal{C}^{(1)}$. □

The following result can be used to determine that a path of solution does not undergo any secondary bifurcations.

Corollary 2. *Consider T_s defined by (11) and assume that the hypotheses* (14) *of Theorem 4 and* (15) *of Theorem 5 are satisfied. Then for every $s \in [0,1]$, $\dim\left(Ker\left(Df\left(\tilde{U}(s)\right)\right)\right) = 1$, that is $\tilde{U}(s)$ is a regular path (where $s \mapsto \tilde{U}(s)$ is defined in Theorem 3).*

Proof. According to (12), we have that

$$\sup_{V,V' \in B(0,r)} \left|\left[DT_s\left(\overline{U}_s + V\right)(V')\right]_n\right| \leq Z_n(r,s) \text{ and } \sup_{V,V' \in B(0,r)} \left|\left[DT_s\left(\overline{U}_s + V\right)(V')\right]_d\right| \leq Z_d(r,s).$$

Since $\tilde{U}(s) \in B(\overline{U}_s, r)$, we get that

$$\sup_{\tilde{V} \in B(0,1)} \left|\left[DT_s\left(\tilde{U}(s)\right)\left(\tilde{V}\right)\right]_n\right| \leq \frac{Z_n(r,s)}{r} \text{ and } \sup_{\tilde{V} \in B(0,1)} \left|\left[DT_s\left(\tilde{U}(s)\right)\left(\tilde{V}\right)\right]_d\right| \leq \frac{Z_d(r,s)}{r}.$$

Hence

$$\left\|DT_s\left(\tilde{U}(s)\right)\right\|_q \leq \frac{\|Z(r,s)\|_q}{r} \leq \frac{\|Z(r,s)+Y(r,s)\|_q}{r} < 1,$$

because Y and Z have non negative entries and (14) holds. So we have that

$$\left\|I - JDF_s\left(\tilde{U}(s)\right)\right\|_q < 1.$$

We get that $JDF_s\left(\tilde{U}(s)\right)$ is invertible (its inverse is given by $\sum_{k=0}^{\infty}\left(I - JDF_s(\tilde{U}(s))\right)^k$), and so $DF_s\left(\tilde{U}(s)\right)$ is injective. Let us show that for every $s \in [0,1]$, $\dim\left(Ker\left(Df\left(\tilde{U}(s)\right)\right)\right) = 1$.

Suppose by contradiction that $\dim\left(Ker\left(Df\left(\tilde{U}(s)\right)\right)\right) > 1$. Let $U, V \in \Omega_q$ two linearly independent non-trivial vectors such that $Df\left(\tilde{U}(s)\right)(U) = Df\left(\tilde{U}(s)\right)(V) = 0$. Since $DF_s\left(\tilde{U}(s)\right)$ is injective,

$$DF_s\left(\tilde{U}(s)\right)(U) = \begin{pmatrix} DE_s\left(\tilde{U}(s)\right)(U) \\ Df\left(\tilde{U}(s)\right)(U) \end{pmatrix} = \begin{pmatrix} \dot{U}_s \cdot U \\ 0 \end{pmatrix} \neq 0.$$

Hence, $\dot{U}_s \cdot U \neq 0$ and $\dot{U}_s \cdot V \neq 0$, and then we can define $W = \dfrac{U}{\dot{U}_s \cdot U} - \dfrac{V}{\dot{U}_s \cdot V} \neq 0$. We conclude that $DF_s\left(\tilde{U}(s)\right)(W) = 0$. This is a contradiction. Hence $\dim\left(Ker\left(Df\left(\tilde{U}(s)\right)\right)\right) \leq 1$. The derivative of the relation $f\left(\tilde{U}(s)\right) = 0$ with respect to s is given by

$$Df(\tilde{U}(s))\left(\frac{d\tilde{U}}{ds}(s)\right) = 0.$$

We showed in the proof of Theorem 5 since (15) holds, that $\dfrac{d\tilde{U}}{ds}(s) \neq 0$. Hence, for every $s \in [0,1]$, $\dim\left(Ker\left(Df\left(\tilde{U}(s)\right)\right)\right) = 1$, meaning by definition that $\tilde{U}(s)$ is a regular path. $\square$

3 Application to a 3-component reaction-diffusion PDEs

In this section, we present all quantities and estimates to construct explicitly the radii polynomials required to apply the theory of the general method of Section 2 to the problem of computing rigorously global smooth branches of steady states of the system of three reaction-diffusion PDEs given by (1). The first step is to consider a Galerkin projection of f given in (3).

3.1 Finite dimensional projection

Given a finite dimensional parameter m, denote $x^{[m]} \in \mathbb{R}^m$ to be $(x_0, \dots, x_{m-1})$ and $u^{[m]} \in \mathbb{R}^{3m}$ to be $(x_0, y_0, z_0, \dots, x_{m-1}, y_{m-1}, z_{m-1})$. The finite dimensional Galerkin projection of f is

$$f^{[m]} \overset{\text{def}}{=} \begin{cases} \mathbb{R} \times \mathbb{R}^{3m} \longrightarrow \mathbb{R}^{3m} \\ U^{[m]} \overset{\text{def}}{=} \left(d, u^{[m]}\right) \longmapsto \left(f_0^{[m]}\left(U^{[m]}\right), \dots, f_{m-1}^{[m]}\left(U^{[m]}\right)\right), \end{cases}$$

where for $n \in \{0, \dots, m-1\}$,

$$\begin{aligned}
f_{n_x}^{[m]}\left(U^{[m]}\right) &= (r_1 - d(\pi n)^2)x_n + \frac{1}{\varepsilon}y_n - \frac{a_1}{2}\sum_{\substack{|k|<m \\ |n-k|<m}} x_{|n-k|}x_{|k|} - \frac{a_1}{2}\sum_{\substack{|k|<m \\ |n-k|<m}} x_{|n-k|}y_{|k|} \\
&- \left(\frac{b_1}{2} + \frac{1}{2\varepsilon N}\right)\sum_{\substack{|k|<m \\ |n-k|<m}} x_{|n-k|}z_{|k|} - \frac{1}{2\varepsilon N}\sum_{\substack{|k|<m \\ |n-k|<m}} y_{|n-k|}z_{|k|}, \\
f_{n_y}^{[m]}\left(U^{[m]}\right) &= \left((r_1 - \frac{1}{\varepsilon} - (d+\beta N)(\pi n)^2)y_n - \frac{a_1}{2}\sum_{\substack{|k|<m \\ |n-k|<m}} y_{|n-k|}y_{|k|} - \frac{a_1}{2}\sum_{\substack{|k|<m \\ |n-k|<m}} x_{|n-k|}y_{|k|}\right. \\
&- \left(\frac{b_1}{2} - \frac{1}{2\varepsilon N}\right)\sum_{\substack{|k|<m \\ |n-k|<m}} y_{|n-k|}z_{|k|} + \frac{1}{2\varepsilon N}\sum_{\substack{|k|<m \\ |n-k|<m}} x_{|n-k|}z_{|k|}, \\
f_{n_z}^{[m]}\left(U^{[m]}\right) &= (r_2 - d(\pi n)^2)z_n - \frac{a_2}{2}\sum_{\substack{|k|<m \\ |n-k|<m}} z_{|n-k|}z_{|k|} \\
&- \frac{b_2}{2}\sum_{\substack{|k|<m \\ |n-k|<m}} x_{|n-k|}z_{|k|} - \frac{b_2}{2}\sum_{\substack{|k|<m \\ |n-k|<m}} y_{|n-k|}z_{|k|} = 0.
\end{aligned} \tag{17}$$

3.2 Explicit construction of the contraction T_s

To define the Newton-like operator T_s given in (11), remember that we have to build an injective linear operator J which approximates the inverse of $DF_0\left(\overline{U}_0\right)$ (with $\overline{U}_0$ an approximate zero of f given by a predictor-corrector step). Since

$$DF_0\left(\overline{U}_0\right) = \left(\begin{array}{c|c} \left(\dot{U}_0\right)^T & \\ \hline \frac{\partial f}{\partial d}\left(\overline{U}_0\right) & D_u f\left(\overline{U}_0\right) \\ & \end{array}\right),$$

we take

$$J = \begin{pmatrix} J^{[m]} & & 0 & \\ & J_m & & \\ 0 & & J_{m+1} & \\ & & & \ddots \end{pmatrix}, \tag{18}$$

where $J^{[m]}$ is a numerical inverse of $DF_0^{[m]}\left(\overline{U}^{[m]}\right)$ that is

$$J^{[m]} \approx \left(\begin{array}{c|c} \left(\dot{U}_0^{[m]}\right)^T & \\ \hline \frac{\partial f^{[m]}}{\partial d}\left(\overline{U}_0^{[m]}\right) & D_u f^{[m]}\left(\overline{U}_0^{[m]}\right) \\ & \end{array}\right)^{-1},$$

and J_n ($n \geq m$) is a 3×3 matrix defined as

$$\begin{aligned} J_n &= \begin{pmatrix} r_1 - d(\pi n)^2 & \frac{1}{\varepsilon} & 0 \\ 0 & r_1 - \frac{1}{\varepsilon} - (d+\beta N)(\pi n)^2 & 0 \\ 0 & 0 & r_2 - d(\pi n)^2 \end{pmatrix}^{-1} \\ &= \begin{pmatrix} \frac{1}{r_1 - d(\pi n)^2} & -\frac{1}{\varepsilon(r_1 - d(\pi n)^2)(r_1 - \frac{1}{\varepsilon} - (d+\beta N)(\pi n)^2)} & 0 \\ 0 & \frac{1}{r_1 - \frac{1}{\varepsilon} - (d+\beta N)(\pi n)^2} & 0 \\ 0 & 0 & \frac{1}{r_2 - d(\pi n)^2} \end{pmatrix}. \end{aligned} \tag{19}$$

J_n is the inverse of the linear part of $f_n(d,\cdot) = (f_{n_x}(d,\cdot), f_{n_y}(d,\cdot), f_{n_z}(d,\cdot))$. The idea behind this choice is explained soon and its interest will appear concretely in Section 3.7.2. To prove that J is really injective, we compute $\left\| I^{[m]} - J^{(m)} DF_0(\overline{U}_0) \right\|_\infty$ using interval arithmetic and check that its value is less than one, and then prove that the matrices J_n ($n \geq m$) are invertible (we only need to check using interval arithmetic that for all $n \geq m$, $r_1 - d(\pi n)^2 \neq 0$ and $r_2 - d(\pi n)^2 \neq 0$, since $r_1 - \frac{1}{\varepsilon} - (d+\beta N)(\pi n)^2 < 0$ with the values of the parameters we are considering).

3.3 Verifying that $T_s(\Omega_q) \subset \Omega_q$ and bootstrap argument

Remark that because of the $(\pi n)^2$ terms, f goes from the space Ω_q to the space $\left\{ u \mid \|u\|_{q-2} < \infty \right\}$. Indeed, since Ω_q is a Banach algebra (see Section 3.5), the non linear terms in f do not affect

the decay rate of $f(U)$. However, thanks to the choice of J_n, J defined by (18) goes from Ω_{q-2} to Ω_q so that $T_s(\Omega_q) \subset \Omega_q$. Remark that if $q \in (1,2)$, we cannot directly conclude that the solution $U \in \Omega_q$ of $f = 0$ is a strong solution of (1). However, since $f(U) = 0$, then (3) becomes

$$\begin{cases} d(\pi n)^2 x_n = r_1 x_n + \dfrac{1}{\varepsilon} y_n - a_1[x^2]_n - a_1[x*y]_n - (b_1 + \dfrac{1}{\varepsilon N})[xz]_n - \dfrac{1}{\varepsilon N}[y*z]_n, \\ (d+\beta N)(\pi n)^2 y_n = ((r_1 - \dfrac{1}{\varepsilon}) y_n - a_1[y^2]_n - a_1[x*y]_n - (b_1 - \dfrac{1}{\varepsilon N})[y*z]_n + \dfrac{1}{\varepsilon N}[x*z]_n, \\ d(\pi n)^2 z_n = r_2 z_n - a_2[z^2]_n - b_2[x*z]_n - b_2[y*z]_n, \end{cases}$$

where each right-hand-side is in Ω_q (here again we use the fact that $(\Omega_q, *)$ is a Banach algebra). One can then easily see by dividing on both sides by $(\pi n)^2$ that U is in fact in Ω_{q+2}. We can repeat this bootstrap argument to prove that any zero U of f lying in some Ω_q ($q > 1$) is in fact in every Ω_{q_0} for $q_0 > 1$ and hence corresponds to C^∞ steady states of (1). Furthermore, the estimates of Section 3.5 can be used to get explicit bounds for derivatives of any order for those solution functions, even if we did the proof with a $q \in (1,2)$.

We are almost ready to compute explicitly the bounds Y and Z and the radii polynomials. But to do so, we need to compute D^2F_s and to bound the convolution product that appear in it. That is what we do in the next two sections.

3.4 Computation of DF_s and D^2F_s

In this section, we use the notation

$$\begin{cases} \overline{U}_0 = (\overline{d}, \overline{x}_0, \overline{y}_0, \overline{z}_0, \dots, \overline{x}_n, \overline{y}_n, \overline{z}_n, \dots), \\ V = (d, x_0, y_0, z_0, \dots, x_n, y_n, z_n, \dots), \\ V' = (d', x_0', y_0', z_0', \dots, x_n', y_n', z_n', \dots). \end{cases}$$

Recall the definition of F_s in (10). First,

$$\left[DF_s(\overline{U}_0)(V)\right]_d = \dot{U}_s \cdot V,$$

and

$$\left[D^2F_s(\overline{U}_0)(V)(V')\right]_d = 0.$$

With the expression of f_n in mind (3), we set

$$L_n(U) = \begin{pmatrix} (r_1 - d(\pi n)^2)x_n + \frac{1}{\varepsilon} y_n \\ ((r_1 - \frac{1}{\varepsilon} - (d+\beta N)(\pi n)^2) y_n \\ (r_2 - d(\pi n)^2) z_n \end{pmatrix}$$

and

$$Q_n(U) = \begin{pmatrix} -a_1[x^2]_n - a_1[x*y]_n - (b_1 + \frac{1}{\varepsilon N})[x*z]_n - \frac{1}{\varepsilon N}[y*z]_n \\ -a_1[y^2]_n - a_1[x*y]_n - (b_1 - \frac{1}{\varepsilon N})[y*z]_n + \frac{1}{\varepsilon N}[x*z]_n \\ -a_2[z^2]_n - b_2[x*z]_n - b_2[y*z]_n \end{pmatrix},$$

so that $f_n = L_n + Q_n$. Then we have

$$\left[DF_s(\overline{U}_0)(V)\right]_n = Df_n(\overline{U}_0)(V) = D_d L_n(\overline{U}_0)(d) + D_u L_n(\overline{U}_0)(v) + DQ_n(\overline{U}_0)(V) \tag{20}$$

and

$$\begin{aligned}\left[D^2F_s(\overline{U}_0)(V)(V')\right]_n &= D^2f_n(\overline{U}_0)(V)(V') \\ &= D^2_{ud}L_n(\overline{U}_0)(d)(v') + D^2_{du}L_n(\overline{U}_0)(v)(d') + D^2Q_n(\overline{U}_0)(V)(V').\end{aligned} \tag{21}$$

Also, $D^2Q_n(\overline{U}_0)(V)(V') = DQ_n(V)(V')$ because DQ_n is linear (Q_n is quadratic). More explicitly, all terms in (20) and (21) can be recovered from the fact that

$$D_dL_n(\overline{U}_0)(d) = -(\pi n)^2\overline{u}_n d,$$

$$D_uL_n(\overline{U}_0)(v) = \begin{pmatrix} (r_1 - \overline{d}(\pi n)^2)x_n + \frac{1}{\varepsilon}y_n \\ ((r_1 - \frac{1}{\varepsilon} - (\overline{d} + \beta N)(\pi n)^2)y_n \\ (r_2 - \overline{d}(\pi n)^2)z_n \end{pmatrix},$$

$DQ_n(V)(V') =$

$$\begin{pmatrix} -2a_1[x*x']_n - a_1[y*x']_n - (b_1 + \frac{1}{\varepsilon N})[z*x']_n - a_1[x*y']_n - \frac{1}{\varepsilon N}[z*y']_n - b_1[x*z']_n - \frac{1}{\varepsilon N}([x*z']_n + [y*z']_n) \\ -a_1[y*x']_n + \frac{1}{\varepsilon N}[z*x']_n - 2a_1[y*y']_n - a_1[x*y']_n + (\frac{1}{\varepsilon N} - b_1)[z*y']_n - b_1[y*z']_n + \frac{1}{\varepsilon N}([x*z']_n + [y*z']_n) \\ -b_2[z*x']_n - b_2[z*y']_n - 2a_2[z*z']_n - b_2([x*z']_n + [y*z']_n) \end{pmatrix},$$

$$D^2_{ud}L_n(\overline{U}_0)(d)(v') = -(\pi n)^2 dv'_n$$

and

$$D^2_{du}L_n(\overline{U}_0)(v)(d') = -(\pi n)^2 d'v_n.$$

3.5 Analytic estimates

In order to bound all terms in (20) and (21), in particular quantities like $[x*y]_n$, for $n \in \mathbb{N}$, we have to develop some analytic estimates. Similar estimates have been produced for the case $q \geq 2$ (e.g. [15]), but not for the case $q \in (1,2)$. From these estimates, we get that $(\Omega_q, *)$ is a Banach algebra for each $q > 1$. First notice that, for all $x, y \in \Omega_q$,

$$|[x*y]_n|\,\omega_n^q = \frac{1}{2}\omega_n^q \sum_{k\in\mathbb{Z}} x_{|k|}y_{|n-k|} \leq \frac{1}{2}\sum_{k\in\mathbb{Z}} \frac{\omega_n^q}{\omega_k^q\omega_{n-k}^q}\,\|x\|_q\,\|y\|_q\,.$$

Thus, what we need to show is that

$$\Psi_n^q \stackrel{\text{def}}{=} \sum_{k\in\mathbb{Z}} \frac{\omega_n^q}{\omega_k^q\omega_{n-k}^q}$$

is bounded for $n \in \mathbb{N}$. We start by rewriting Ψ_n^q. If $n = 0$,

$$\sum_{k\in\mathbb{Z}} \frac{\omega_n^q}{\omega_k^q\omega_{n-k}^q} = \sum_{k=-\infty}^{-1} \frac{\omega_n^q}{\omega_k^q\omega_{n-k}^q} + 1 + \sum_{k=1}^{\infty} \frac{\omega_n^q}{\omega_k^q\omega_{n-k}^q} = 1 + 2\sum_{k=1}^{\infty} \frac{n^q}{k^q\,(n+k)^q},$$

and if $n > 0$,

$$\begin{aligned}\sum_{k\in\mathbb{Z}} \frac{\omega_n^q}{\omega_k^q\omega_{n-k}^q} &= \sum_{k=-\infty}^{-1} \frac{\omega_n^q}{\omega_k^q\omega_{n-k}^q} + 1 + \sum_{k=1}^{n-1} \frac{\omega_n^q}{\omega_k^q\omega_{n-k}^q} + 1 + \sum_{k=n+1}^{\infty} \frac{\omega_n^q}{\omega_k^q\omega_{n-k}^q} \\ &= 2 + 2\sum_{k=1}^{\infty} \frac{n^q}{k^q\,(n+k)^q} + \sum_{k=1}^{n-1} \frac{n^q}{k^q\,(n-k)^q}.\end{aligned} \tag{22}$$

In everything that follows, K is a computational parameter (the larger K is, the sharper the estimates will, but the greater the computational cost for the evaluation of the estimates will be) and M is another computational parameter (which is taken equal to $2m-1$, see Section 3.6). First we define, for $n \geq 2$

$$\chi_n(q) = \left(\frac{q}{2-q} + \frac{q(q-1)}{2(3-q)} + \frac{q(q-1)}{2\left\lfloor \frac{n}{2} \right\rfloor} + \frac{2-(2/3)^q}{\left\lfloor \frac{n}{2} \right\rfloor} - \frac{2-(2/3)^q}{q-1} \right) \frac{1}{\left\lfloor \frac{n}{2} \right\rfloor^{q-1}}, \tag{23}$$

and $q^*(M)$ the unique zero of χ_M in $(1,2)$. Note that χ_M is increasing on $(1,2)$, goes to $-\infty$ as q goes to 1 and to ∞ as q goes to 2, so $q^*(M)$ is well defined. Then we define

$$\gamma_M^q(K) \stackrel{\text{def}}{=} \begin{cases} 2\sum_{k=1}^{K} \frac{1}{k^q} + \frac{2}{(q-1)K^{q-1}}, & \text{if } 1 < q < q^*(M) \\ 2\sum_{k=1}^{K} \frac{1}{k^q} + \frac{2}{(q-1)K^{q-1}} + 2\chi_M(q), & \text{if } q^*(M) \leq q < 2 \\ 2\left(\frac{M}{M-1}\right)^q + \left(\frac{4\ln(M-2)}{M} + \frac{\pi^2-6}{3}\right)\left(\frac{2}{M}+\frac{1}{2}\right)^{q-2}, & \text{if } q \geq 2, \end{cases}$$

and finally

$$\alpha_n^q(K) \stackrel{\text{def}}{=} \begin{cases} 1 + 2\sum_{k=1}^{K} \frac{1}{k^q} + \frac{2}{(q-1)K^{q-1}}, & \text{if } n = 0 \\ 2 + 2\sum_{k=1}^{K} \frac{1}{k^q} + \frac{2}{(q-1)K^{q-1}} + \sum_{k=1}^{n-1} \frac{n^q}{k^q\,(n-k)^q}, & \text{if } 1 \leq n < M \\ 2 + 2\sum_{k=1}^{K} \frac{1}{k^q} + \frac{2}{(q-1)K^{q-1}} + \gamma_M^{(q)}, & \text{if } n \geq M. \end{cases} \tag{24}$$

Proposition 1. *Let $q > 1$, K and $M \geq 6$ computational parameters. For all $n \in \mathbb{N}$,*

$$\Psi_n^q \leq \alpha_n^q(K).$$

This allows us to state the following result.

Lemma 3. *Let $x, y \in \Omega_q$, $q > 1$, K and $M \geq 6$ computational parameters. For all $n \geq M$,*

$$|[x * y]_n| \leq \frac{1}{2} \frac{\alpha_M^q(K)}{\omega_n^q} \|x\|_q \|y\|_q .$$

This bound, in addition of being very useful later in this paper, proves that $(\Omega_q, *)$ is a Banach algebra for $q > 1$.

Proof. (of Proposition 1) The bound for $q \geq 2$ is due to [15]. We prove the bound for $q < 2$. The case $n < M$ is a direct consequence of the following inequality applied to (22)

$$\sum_{k=1}^{\infty} \frac{n^q}{k^q\,(n+k)^q} \leq \sum_{k=1}^{\infty} \frac{1}{k^q} \leq \sum_{k=1}^{K} \frac{1}{k^q} + \frac{1}{(q-1)K^{q-1}}.$$

For the case $n \geq M$, let us consider the difference

$$\Delta_n^q \stackrel{\text{def}}{=} \Psi_n^q - \left(2 + 4\sum_{k=1}^{\infty} \frac{1}{k^q}\right).$$

Using (22) and the inequality below

$$\begin{aligned}\sum_{k=1}^{n-1}\frac{n^q}{k^q(n-k)^q} &= \sum_{k=1}^{\lfloor\frac{n}{2}\rfloor}\frac{n^q}{k^q(n-k)^q}+\sum_{k=\lfloor\frac{n}{2}\rfloor+1}^{n-1}\frac{n^q}{k^q(n-k)^q}\\ &= \sum_{k=1}^{\lfloor\frac{n}{2}\rfloor}\frac{n^q}{k^q(n-k)^q}+\sum_{l=1}^{n-\lfloor\frac{n}{2}\rfloor-1}\frac{n^q}{l^q(n-l)^q} \qquad \text{(we set } l=n-k)\\ &\leq 2\sum_{k=1}^{\lfloor\frac{n}{2}\rfloor}\frac{n^q}{k^q(n-k)^q} \qquad \left(n-\left\lfloor\frac{n}{2}\right\rfloor-1\leq\left\lfloor\frac{n}{2}\right\rfloor\right),\end{aligned}$$

we get that

$$\begin{aligned}\Delta_n^q &\leq 2\left(\sum_{k=1}^{\infty}\frac{1}{k^q}\left(\frac{n^q}{(n+k)^q}-1\right)+\sum_{k=1}^{\lfloor\frac{n}{2}\rfloor}\frac{1}{k^q}\left(\frac{n^q}{(n-k)^q}-1\right)-\sum_{k=\lfloor\frac{n}{2}\rfloor+1}^{\infty}\frac{1}{k^q}\right)\\ &\leq 2\left(\sum_{k=1}^{\lfloor\frac{n}{2}\rfloor}\frac{1}{k^q}\left(\frac{n^q}{(n-k)^q}-1\right)-\left(2-\left(\frac{2}{3}\right)^q\right)\sum_{k=\lfloor\frac{n}{2}\rfloor+1}^{\infty}\frac{1}{k^q}\right). \qquad (25)\end{aligned}$$

The first term of (25) can be bounded from above as follows

$$\begin{aligned}\sum_{k=1}^{\lfloor\frac{n}{2}\rfloor}\frac{1}{k^q}\left(\frac{n^q}{(n-k)^q}-1\right) &= \sum_{k=1}^{\lfloor\frac{n}{2}\rfloor}\frac{1}{k^q}\left(\left(1+\frac{k}{(n-k)}\right)^q-1\right)\\ &= \sum_{k=1}^{\lfloor\frac{n}{2}\rfloor}\frac{1}{k^q}\sum_{l=1}^{\infty}\frac{q(q-1)\dots(q-l+1)}{l!}\frac{k^l}{(n-k)^l}\\ &\leq \sum_{k=1}^{\lfloor\frac{n}{2}\rfloor}\frac{1}{k^q}\left(q\frac{k}{(n-k)}+\frac{q(q-1)}{2}\frac{k^2}{(n-k)^2}\right). \qquad (26)\end{aligned}$$

The last inequality is due to the fact that for all $u\in(0,1)$, the series expansion

$$(1+u)^q=1+\sum_{k=1}^{\infty}\frac{q(q-1)\dots(q-k+1)}{k!}u^k$$

is an alternating series for $k\geq 2$ (recall that $q\in(1,2)$). According to (26), we have to bound $\sum_{k=1}^{\lfloor\frac{n}{2}\rfloor}\frac{q}{k^q}\frac{k}{(n-k)}$ and $\sum_{k=1}^{\lfloor\frac{n}{2}\rfloor}\frac{q(q-1)}{2k^q}\frac{k^2}{(n-k)^2}$. First,

$$\sum_{k=1}^{\lfloor\frac{n}{2}\rfloor}\frac{1}{k^{q-1}}\leq 1+\int_1^{\lfloor\frac{n}{2}\rfloor}\frac{dt}{t^{q-1}}=1+\frac{1}{2-q}\left(\left\lfloor\frac{n}{2}\right\rfloor^{2-q}-1\right)\leq\frac{1}{2-q}\left\lfloor\frac{n}{2}\right\rfloor^{2-q},$$

and then,

$$\sum_{k=1}^{\lfloor\frac{n}{2}\rfloor}\frac{q}{k^q}\frac{k}{(n-k)}\leq\frac{q}{\lfloor\frac{n}{2}\rfloor}\sum_{k=1}^{\lfloor\frac{n}{2}\rfloor}\frac{1}{k^{q-1}}\leq\frac{q}{2-q}\frac{1}{\lfloor\frac{n}{2}\rfloor^{q-1}}. \qquad (27)$$

Similarly

$$\sum_{k=1}^{\lfloor\frac{n}{2}\rfloor}k^{2-q}\leq\int_1^{\lfloor\frac{n}{2}\rfloor}t^{2-q}dt+\left\lfloor\frac{n}{2}\right\rfloor^{2-q}=\frac{1}{3-q}\left(\left\lfloor\frac{n}{2}\right\rfloor^{3-q}-1\right)+\left\lfloor\frac{n}{2}\right\rfloor^{2-q}\leq\frac{1}{3-q}\left\lfloor\frac{n}{2}\right\rfloor^{3-q}+\left\lfloor\frac{n}{2}\right\rfloor^{2-q},$$

and then

$$\sum_{k=1}^{\lfloor \frac{n}{2} \rfloor} \frac{q(q-1)}{2k^q} \frac{k^2}{(n-k)^2} \leq \frac{q(q-1)}{2\left\lfloor \frac{n}{2} \right\rfloor^2} \sum_{k=1}^{\lfloor \frac{n}{2} \rfloor} k^{2-q} \leq \frac{q(q-1)}{2\left\lfloor \frac{n}{2} \right\rfloor^{q-1}} \left(\frac{1}{3-q} + \frac{1}{\lfloor \frac{n}{2} \rfloor} \right). \tag{28}$$

According to (26), (27) and (28), we get

$$\sum_{k=1}^{\lfloor \frac{n}{2} \rfloor} \frac{1}{k^q} \left(\frac{n^q}{(n-k)^q} - 1 \right) \leq \left(\frac{q(q-1)}{2(3-q)} + \frac{q(q-1)}{2\left\lfloor \frac{n}{2} \right\rfloor} + \frac{q}{2-q} \right) \frac{1}{\left\lfloor \frac{n}{2} \right\rfloor^{q-1}}. \tag{29}$$

Then we bound the second term of (25) from below

$$\sum_{k=\lfloor \frac{n}{2} \rfloor+1}^{\infty} \frac{1}{k^q} = \sum_{k=\lfloor \frac{n}{2} \rfloor}^{\infty} \frac{1}{k^q} - \frac{1}{\left\lfloor \frac{n}{2} \right\rfloor^q} \geq \int_{\lfloor \frac{n}{2} \rfloor}^{\infty} \frac{dt}{t^q} - \frac{1}{\left\lfloor \frac{n}{2} \right\rfloor^q} = \frac{1}{q-1} \frac{1}{\left\lfloor \frac{n}{2} \right\rfloor^{q-1}} - \frac{1}{\left\lfloor \frac{n}{2} \right\rfloor^q}. \tag{30}$$

Using (25), (29) and (30) , we get

$$\Delta_n^q \leq 2 \left(\frac{q(q-1)}{2(3-q)} + \frac{q(q-1)}{2\left\lfloor \frac{n}{2} \right\rfloor} + \frac{q}{2-q} + \frac{1}{\lfloor \frac{n}{2} \rfloor} - \frac{1}{q-1} \right) \frac{1}{\left\lfloor \frac{n}{2} \right\rfloor^{q-1}} = 2\chi_n(q). \tag{31}$$

Now, if $q < q^*(M)$ then $\chi_M(q) < 0$ and hence for all $n \geq M$, $\chi_n(q) < 0$. Thus

$$\Psi_n^q \leq 2 + 4 \sum_{k=1}^{\infty} \frac{1}{k^q} \leq 2 + 4 \sum_{k=1}^{K} \frac{1}{k^q} + \frac{4}{(q-1)K^{q-1}}.$$

If $q \geq q^*(M)$ then $\chi_M(q) \geq 0$ and we have two cases. The first case is that $\chi_n(q)$ decreases until becoming negative for some $n_0 > M$ which implies that $\chi_n(q) < 0$ for all $n \geq n_0$. The second case is that $\chi_n(q)$ stays positive for all $n \geq M$ which implies that $\chi_n(q)$ is decreasing for all $n \geq M$. In both cases we get that $\chi_n(q) \leq \chi_M(q)$ for all $n \geq M$ and thus

$$\Psi_n^q \leq 2 + 4 \sum_{k=1}^{\infty} \frac{1}{k^q} + 2\chi_M(q) \leq 2 + 4 \sum_{k=1}^{K} \frac{1}{k^q} + \frac{4}{(q-1)K^{q-1}} + 2\chi_M(q).$$

□

Notice that since $\lim_n \chi_n(q) = 0$, (31) shows that $\limsup_n \Delta_n^q \leq 0$. We could do the same kind of computation to bound Δ_n^q from below and show that in fact $\lim_n \Delta_n^q = 0$. So the bound for $q < q^*(M)$ is optimal, the only thing that can be improved is the way we approximate $\sum_{k=1}^{\infty} \frac{1}{k^q}$ (which depends of K). But this also shows that the bound for $q^*(M) \leq q < 2$ may not be optimal, in fact it becomes quite bad when q is close to 2 since $\lim_{q \to 2} \chi_M(q) = \infty$. However, if sharp estimates are needed for q close to 2, there is a numerical way to get almost optimal bounds which is detailed it in Appendix A.1. We now give other bounds that are sharper for $n < M$ by using computations. Let us define

$$C_n^q(K) \stackrel{\text{def}}{=} \sum_{\substack{n_1+n_2=n \\ |n_1|,|n_2|<K}} \frac{1}{\omega_{n_1}^q} \frac{1}{\omega_{n_2}^q},$$

and

$$\epsilon_n^q(K) \stackrel{\text{def}}{=} \frac{2}{(q-1)(K-1)^{q-1}} \left(\frac{1}{(K-n)^q} + \frac{1}{(K+n)^q} \right).$$

Lemma 4 (Sharper estimates)**.** *Let $x, y \in \Omega_q$, $q > 1$, K and M computational parameters, $M \leq K$. for all $n < M$*

$$|[x * y]_n| \leq \frac{1}{2} \left(C_n^q(K) + \epsilon_n^q(K)\right) \|x\|_q \|y\|_q ,$$

Proof.

$$|[x * y]_n| \leq \frac{1}{2} \left(\sum_{n_1+n_2=n} \frac{1}{\omega_{n_1}^q} \frac{1}{\omega_{n_2}^q} \right) \|x\|_q \|y\|_q .$$

We can split the summation in two parts :

$$\sum_{n_1+n_2=n} \frac{1}{\omega_{n_1}^q} \frac{1}{\omega_{n_2}^q} = \sum_{\substack{n_1+n_2=n \\ |n_1|,|n_2|<K}} \frac{1}{\omega_{n_1}^q} \frac{1}{\omega_{n_2}^q} + \sum_{\substack{n_1+n_2=n \\ \max(|n_1|,|n_2|)\geq K}} \frac{1}{\omega_{n_1}^q} \frac{1}{\omega_{n_2}^q}.$$

The first one is exactly $C_n^q(K)$. We now bound the second one :

$$\begin{aligned}
\sum_{\substack{n_1+n_2=n \\ \max(|n_1|,|n_2|)\geq K}} \frac{1}{\omega_{n_1}^q} \frac{1}{\omega_{n_2}^q} &\leq 2 \sum_{\substack{n_1+n_2=n \\ |n_1|\geq K}} \frac{1}{\omega_{n_1}^q} \frac{1}{\omega_{n_2}^q} \\
&\leq 2 \sum_{n_1=K}^{\infty} \frac{1}{\omega_{n_1}^q} \left(\frac{1}{\omega_{n-n_1}^q} + \frac{1}{\omega_{n+n_1}^q} \right) \\
&\leq \frac{2}{(q-1)(K-1)^{q-1}} \left(\frac{1}{(K-n)^q} + \frac{1}{(K+n)^q} \right).
\end{aligned}$$

□

Remark 1. *$q^*(M)$, the unique zero of χ_M in $(1, 2)$ defined in (23), is increasing in M and converges rather rapidly towards a bounded value. In particular, for $M \geq 100$ (which is always the case for the proofs presented in this work), one has that $q^*(M) \geq q^*(100) = 1.4730$. Numerically, the limit when M goes to ∞ is about 1.475.*

3.6 Computation of Y_n

According to (12), we focus here on

$$\left| T_s\left(\overline{U}_s\right) - \overline{U}_s \right| = \left| JF_s\left(\overline{U}_s\right) \right| \leq |J| \left| F_s\left(\overline{U}_s\right) \right|.$$

Remember that absolute values and inequalities applied to vectors or matrices should be understood component wise. Observe that $E_s(\overline{U}_s) = 0$ so that

$$F_s\left(\overline{U}_s\right) = \begin{pmatrix} 0 \\ f\left(\overline{U}_s\right) \end{pmatrix}.$$

Because of the shape of J in (18), we compute separately the bounds for $n < m$ and $n \geq m$.

3.6.1 Case $n < m$

Following the notation introduced earlier, $Y^{[m]}$ is the vector containing Y_d and Y_n for any $n < m$. We want to bound the quantity

$$\left| J^{[m]} \right| \left| \begin{pmatrix} 0 \\ f^{[m]}\left(\overline{U}_s\right) \end{pmatrix} \right|.$$

With the expression $\overline{U}_s = \overline{U}_0 + s\Delta\overline{U}$ and a Taylor expansion, we get that

$$f^{[m]}\left(\overline{U}_s^{[m]}\right) = f^{[m]}\left(\overline{U}_0^{[m]}\right) + sDf^{[m]}\left(\overline{U}_0^{[m]}\right)\left(\Delta\overline{U}^{[m]}\right) + \frac{s^2}{2}D^2f^{[m]}\left(\overline{U}_0^{[m]}\right)\left(\Delta\overline{U}^{[m]}\right)^2,$$

which can be bounded, for $s \in [0,1]$, by

$$\tilde{f}^{[m]} \stackrel{\text{def}}{=} \left|f^{[m]}\left(\overline{U}_0^{[m]}\right)\right| + s\left|Df^{[m]}\left(\overline{U}_0^{[m]}\right)\left(\Delta\overline{U}^{[m]}\right)\right| + \frac{s^2}{2}\left|D^2f^{[m]}\left(\overline{U}_0^{[m]}\right)\left(\Delta\overline{U}^{[m]}\right)^2\right|.$$

We see in Section 3.8 that we can get a uniform bound in s by taking $s = 1$ in the expression above. This uniform bound is simple to get but not the sharpest. We actually show in Appendix A.2 how to compute a sharper bound. The vectors $Df^{[m]}\left(\overline{U}_0^{[m]}\right)\left(\Delta\overline{U}^{[m]}\right)$ and $D^2f^{[m]}\left(\overline{U}_0^{[m]}\right)\left(\Delta\overline{U}^{[m]}\right)^2$ are computed with the expressions (20) and (21) by truncating the convolution products as in (17). This is a finite computation. We can set

$$Y^{[m]} \stackrel{\text{def}}{=} \left|J^{[m]}\right|\begin{pmatrix}0\\ \tilde{f}^{[m]}\end{pmatrix}.$$

3.6.2 Case $n \geq m$

For $n \geq m$,

$$\left|\left[T_s(\overline{U}_s) - \overline{U}_s\right]_n\right| = \left|J_nf_n(\overline{U}_s)\right| = \left|J_n\left(f_n(\overline{U}_0) + sDf_n(\overline{U}_0)(\Delta\overline{U}) + \frac{s^2}{2}D^2f_n(\overline{U}_0)(\Delta\overline{U})^2\right)\right|.$$

We can then set

$$Y_n \stackrel{\text{def}}{=} |J_n|\left(\left|f_n(\overline{U}_0)\right| + s\left|Df_n(\overline{U}_0)(\Delta\overline{U})\right| + \frac{s}{2}\left|D^2f_n(\overline{U}_0)(\Delta\overline{U})^2\right|\right).$$

The terms $Df_n\left(\overline{U}_0\right)\left(\Delta\overline{U}\right)$ and $D^2f_n\left(\overline{U}_0\right)\left(\Delta\overline{U}\right)^2$ are computed with the expressions (20) and (21). We can compute Y_n in a finite number of operations, because for any $n \geq m$, $\left[\overline{U}_0\right]_n = 0$ and $\left[\Delta\overline{U}\right]_n = 0$. In particular, for any $n \geq 2m-1$, $f_n(\overline{U}_s) = 0$ and we can take $Y_n = 0$, so only a finite number of Y_n remains to be computed. Hence, setting $M = 2m-1$, we have that for all $n \geq M$, $Y_n = 0$. In the next section, we see that for all $n \geq M$, we can set $Z_n = \hat{Z}_M\frac{\omega_M^q}{\omega_n^q}$. In fact, the value of M is determined by the degree of the non linearities of f. Here we have quadratic terms like

$$[\overline{x} * \overline{y}]_n = \sum_{k=n-m+1}^{m-1}\overline{x}_k\overline{y}_{n-k} = 0 \text{ for } n \geq M = 2m-1,$$

and with non linearities of degree p, we would have the same by taking $M = p(m-1)+1$.

3.7 Computation of Z_n

For $V, V' \in B(0,r)$ and $s \in [0,1]$, using a Taylor expansion, we get

$$\begin{aligned} DT_s(\overline{U}_s + V)(V') &= \left(I - JDF_s(\overline{U}_0 + s\Delta\overline{U} + V)\right)(V') \\ &= \left(I - J\left(DF_s(\overline{U}_0) + D^2F_s(\overline{U}_0)(s\Delta\overline{U} + V)\right)\right)(V'). \end{aligned} \tag{32}$$

As for Y, we compute separately the bounds for $n < m$ and $n \geq m$.

3.7.1 Case $n < m$

For all $V' \in B(0,r)$, the shape of J in (18) allows us to write

$$\begin{aligned}
\left[\left(I - JDF_s(\overline{U}_0)\right)(V')\right]^{[m]} &= V'^{[m]} - \left[JDF_s(\overline{U}_0)(V')\right]^{[m]} \\
&= V'^{[m]} - J^{[m]}\left[DF_s(\overline{U}_0)(V')\right]^{[m]} \\
&= V'^{[m]} - J^{[m]}\left(DF_s^{[m]}(\overline{U}_0)\left(V'^{[m]}\right) + R^{[m]}(\overline{U}_0, V')\right) \\
&= \left(I^{[m]} - J^{(m)}DF_s^{[m]}(\overline{U}_0^{[m]})\right)\left(V'^{[m]}\right) - J^{(m)}R^{[m]}(\overline{U}_0, V') \\
&= \left(I^{[m]} - J^{[m]}\left(DF_0^{[m]}(\overline{U}_0^{[m]}) + s\begin{pmatrix}\left(\Delta\dot{U}\right)^T \\ 0\end{pmatrix}\right)\right)\left(V'^{[m]}\right) \\
&\quad -J^{(m)}R^{[m]}(\overline{U}_0, V'), \qquad (33)
\end{aligned}$$

where

$$R_d^{[m]}(\overline{U}_0, V') = \sum_{k=m}^{\infty}\frac{\partial E_s}{\partial x_k}(\overline{U}_0)x'_k + \sum_{k=m}^{\infty}\frac{\partial E_s}{\partial y_k}(\overline{U}_0)y'_k + \sum_{k=m}^{\infty}\frac{\partial E_s}{\partial z_k}(\overline{U}_0)z'_k = 0,$$

and for all $n \in \{0, \ldots, m-1\}$,

$$\begin{aligned}
R_{n_x}^{[m]}(\overline{U}_0, V') &= \sum_{k=m}^{\infty}\frac{\partial f_{n_x}}{\partial x_k}(\overline{U}_0)x'_k + \sum_{k=m}^{\infty}\frac{\partial f_{n_x}}{\partial y_k}(\overline{U}_0)y'_k + \sum_{k=m}^{\infty}\frac{\partial f_{n_x}}{\partial z_k}(\overline{U}_0)z'_k \\
&= -a_1\sum_{k=m}^{m+n-1}\overline{x}_{k-n}x'_k - \frac{a_1}{2}\sum_{k=m}^{m+n-1}\overline{y}_{k-n}x'_k - \frac{1}{2}(b_1 + \frac{1}{\varepsilon N})\sum_{k=m}^{m+n-1}\overline{z}_{k-n}x'_k \\
&\quad -\frac{a_1}{2}\sum_{k=m}^{m+n-1}\overline{x}_{k-n}y'_k - \frac{1}{2\varepsilon N}\sum_{k=m}^{m+n-1}\overline{z}_{k-n}y'_k \\
&\quad -\frac{1}{2}(b_1 + \frac{1}{\varepsilon N})\sum_{k=m}^{m+n-1}\overline{x}_{k-n}z'_k - \frac{1}{2\varepsilon N}\sum_{k=m}^{m+n-1}\overline{y}_{k-n}z'_k.
\end{aligned}$$

Similarly,

$$\begin{aligned}
R_{n_y}^{[m]}(\overline{U}_0, V') &= -a_1\sum_{k=m}^{m+n-1}\overline{y}_{k-n}y'_k - \frac{a_1}{2}\sum_{k=m}^{m+n-1}\overline{x}_{k-n}y'_k - \frac{1}{2}(b_1 - \frac{1}{\varepsilon N})\sum_{k=m}^{m+n-1}\overline{z}_{k-n}y'_k \\
&\quad -\frac{a_1}{2}\sum_{k=m}^{m+n-1}\overline{y}_{k-n}x'_k + \frac{1}{2\varepsilon N}\sum_{k=m}^{m+n-1}\overline{z}_{k-n}x'_k \\
&\quad -\frac{1}{2}(b_1 - \frac{1}{\varepsilon N})\sum_{k=m}^{m+n-1}\overline{y}_{k-n}z'_k + \frac{1}{2\varepsilon N}\sum_{k=m}^{m+n-1}\overline{x}_{k-n}z'_k,
\end{aligned}$$

and

$$\begin{aligned}
R_{n_z}^{[m]}(\overline{U}_0, V') &= -\frac{b_2}{2}\sum_{k=m}^{m+n-1}\overline{z}_{k-n}x'_k - \frac{b_2}{2}\sum_{k=m}^{m+n-1}\overline{z}_{k-n}y'_k \\
&\quad -a_2\sum_{k=m}^{m+n-1}\overline{z}_{k-n}z'_k - \frac{b_2}{2}\sum_{k=m}^{m+n-1}\overline{x}_{k-n}z'_k - \frac{b_2}{2}\sum_{k=m}^{m+n-1}\overline{y}_{k-n}z'_k.
\end{aligned}$$

$R^{[m]}(\overline{U}_0, V')$ can be bounded uniformly for $V' \in B(0,r)$ by $\tilde{R}^{[m]}(\overline{U}_0)r$ where

$$\tilde{R}_d^{[m]}(\overline{U}_0) \stackrel{\text{def}}{=} 0,$$

$$\tilde{R}^{[m]}_{n_x}(\overline{U}_0) \stackrel{\text{def}}{=} \frac{1}{2}\sum_{k=m}^{m+n-1}\left((3a_1+b_1+\frac{1}{\varepsilon N})|\overline{x}_{k-n}|+(a_1+\frac{1}{\varepsilon N})|\overline{y}_{k-n}|+(b_1+\frac{2}{\varepsilon N})|\overline{z}_{k-n}|\right)\frac{1}{\omega^q_k},$$

$$\tilde{R}^{[m]}_{n_y}(\overline{U}_0) \stackrel{\text{def}}{=} \frac{1}{2}\sum_{k=m}^{m+n-1}\left((a_1+\frac{1}{\varepsilon N})|\overline{x}_{k-n}|+(3a_1+b_1+\frac{1}{\varepsilon N})|\overline{y}_{k-n}|+(b_1+\frac{2}{\varepsilon N})|\overline{z}_{k-n}|\right)\frac{1}{\omega^q_k},$$

$$\tilde{R}^{[m]}_{n_z}(\overline{U}_0) \stackrel{\text{def}}{=} \frac{1}{2}\sum_{k=m}^{m+n-1}\left(b_2|\overline{x}_{k-n}|+b_2|\overline{y}_{k-n}|+(2b_2+2a_2)|\overline{z}_{k-n}|\right)\frac{1}{\omega^q_k}.$$

Notice that $\tilde{R}^{[m]}(\overline{U}_0)$ can be computed in a finite number of operations. According to (32) and (33), we have that for all $V, V' \in B(0,r)$,

$$\begin{aligned}\left|DT_s(\overline{U}_s+V)(V')\right| &\leq \left|\left(I^{[m]}-J^{(m)}DF^{[m]}_0(\overline{U}^{[m]}_0)\right)\left(V'^{[m]}\right)\right| + s\left|J^{[m]}\begin{pmatrix}\left(\Delta\dot{U}\right)^T\\0\end{pmatrix}V'^{[m]}\right| \\ &+ \left|J^{(m)}R^{[m]}(\overline{U}_0,V')\right| + |J|\left|D^2F_s(\overline{U}_0)(V)(V')+D^2F_s(\overline{U}_0)(s\Delta U)(V')\right|.\end{aligned}$$

Using expression (21) and Lemma 4, we get that for all $V, V' \in B(0,r)$ and $n < 2m-1$,

$$\left|\left[D^2F_s(\overline{U}_0)(V)(V')\right]_n\right| \leq \frac{1}{2}\left(C^q_n(K)+\epsilon^q_n(K)\right)\begin{pmatrix}\lambda_1\\\lambda_1\\\lambda_2\end{pmatrix}r^2 + \frac{2(\pi n)^2r^2}{\rho\omega^q_n}\begin{pmatrix}1\\1\\1\end{pmatrix}, \tag{34}$$

with $\lambda_1 = 4a_1+2b_1+\dfrac{4}{\varepsilon N}$ and $\lambda_2 = 4b_2+2a_2$. Let us set

$$\widetilde{DQ}^q_n(K) \stackrel{\text{def}}{=} \frac{1}{2}\left(C^q_n(K)+\epsilon^q_n(K)\right)\begin{pmatrix}\lambda_1\\\lambda_1\\\lambda_2\end{pmatrix}.$$

For $\left|\left[D^2F_s(\overline{U}_0)(s\Delta\overline{U})(V')\right]_n\right|$, we know explicitly $\Delta\overline{U}$ which allows us to compute sharper bounds. Still using (21), we get that for all $V' \in B(0,r)$, $s \in [0,1]$ and $n < 2m-1$,

$$\left|\left[D^2F_s(\overline{U}_0)(s\Delta\overline{U})(V')\right]_n\right| \leq s\begin{pmatrix}[\theta_1(\Delta\overline{u})*w^q]_n\\[\theta_2(\Delta\overline{u})*w^q]_n\\[\theta_3(\Delta\overline{u})*w^q]_n\end{pmatrix}r + s(\pi n)^2\begin{pmatrix}\dfrac{|\Delta\overline{d}|}{\omega^q_n}\begin{pmatrix}1\\1\\1\end{pmatrix}r + \dfrac{[|\Delta\overline{u}|]_n}{\rho}r\end{pmatrix}, \tag{35}$$

where

$$\begin{aligned}\theta_1(u) &\stackrel{\text{def}}{=} (3a_1+b_1+\frac{1}{\varepsilon N})|x|+(a_1+\frac{1}{\varepsilon N})|y|+(b_1+\frac{2}{\varepsilon N})|z|,\\ \theta_2(u) &\stackrel{\text{def}}{=} (a_1+\frac{1}{\varepsilon N})|x|+(3a_1+b_1+\frac{1}{\varepsilon N})|y|+(b_1+\frac{2}{\varepsilon N})|z|,\\ \theta_3(u) &\stackrel{\text{def}}{=} b_2|x|+b_2|y|+(2a_2+2b_2)|z|\end{aligned}$$

and

$$w^q \stackrel{\text{def}}{=} \left(\frac{1}{\omega^q_0},\ldots,\frac{1}{\omega^q_n},\ldots\right).$$

Let us also set

$$\Theta_n^q(u) \stackrel{\text{def}}{=} \begin{pmatrix} [\theta_1(u) * w^q]_n \\ [\theta_2(u) * w^q]_n \\ [\theta_3(u) * w^q]_n \end{pmatrix}.$$

Observe that since $\Delta\overline{u}$ has only a finite number of non-zero coefficients, $\Theta_n^q(\Delta\overline{u})$ can be computed in a finite number of operations.

Using all the bounds obtained in this section and the definition of Z in (13), we can define Z_d and the m first Z_n by

$$\begin{aligned} Z^{[m]} &= \left|I^{[m]} - J^{[m]} DF_0^{[m]}(\overline{U}_0^{[m]})\right| (W_1^q)^{[m]}\, r + s \left| J^{[m]} \begin{pmatrix} \left(\Delta\dot{U}\right)^T \\ 0 \end{pmatrix} \right| (W_1^q)^{[m]}\, r + |J^{[m]}| \tilde{R}^{[m]}(\overline{U}_0) r \\ &+ |J^{[m]}| \left(\left(\widetilde{DQ}^q\right)^{[m]} (K) r^2 + \frac{2}{\rho} (W_2^q)^{[m]}\, r^2 + s\, (\Theta^q)^{[m]}\, (\Delta\overline{u}) r + s|\Delta\overline{d}|\, (W_2^q)^{[m]}\, r + \frac{s}{\rho} \Lambda^{[m]}(\Delta\overline{u}) r \right), \end{aligned}$$

where

$$(W_1^q)^{[m]} = \left(\frac{1}{\rho}, \frac{1}{\omega_0^q}, \frac{1}{\omega_0^q}, \frac{1}{\omega_0^q}, \ldots, \frac{1}{\omega_{m-1}^q}, \frac{1}{\omega_{m-1}^q}, \frac{1}{\omega_{m-1}^q} \right)^T,$$

$$(W_2^q)^{[m]} = \left(0, \frac{\pi^2 0^2}{\omega_0^q}, \frac{\pi^2 0^2}{\omega_0^q}, \frac{\pi^2 0^2}{\omega_0^q}, \ldots, \frac{\pi^2 (m-1)^2}{\omega_{m-1}^q}, \frac{\pi^2 (m-1)^2}{\omega_{m-1}^q}, \frac{\pi^2 (m-1)^2}{\omega_{m-1}^q} \right)^T,$$

$$\left(\widetilde{DQ}^q\right)^{[m]} (K) = \begin{pmatrix} 0 \\ \widetilde{DQ}_0^q(K) \\ \vdots \\ \widetilde{DQ}_{m-1}^q(K) \end{pmatrix}, \; (\Theta^q)^{[m]}\, (u) = \begin{pmatrix} 0 \\ \Theta_0^q(u) \\ \vdots \\ \Theta_{m-1}^q(u) \end{pmatrix} \text{ and } \Lambda^{[m]}(u) = \begin{pmatrix} 0 \\ (\pi 0)^2 |u_0| \\ \vdots \\ (\pi(m-1))^2 |u_{m-1}| \end{pmatrix}.$$

3.7.2 Case $m \leq n < M$

Let $m \leq n < 2m-1$. According to (20) we have that

$$\left[DF_s(\overline{U}_0)(V')\right]_n = \underbrace{D_d L_n(\overline{U}_0)(d')}_{=0} + D_u L_n(\overline{U}_0)(v') + DQ_n(\overline{U}_0)(V')$$

and by definition of J_n in (19), $J_n \left(D_u L_n(\overline{U}_0)(v) \right) = v_n$, simplifying (32) into

$$\begin{aligned} \left[DT_s(\overline{U}_s + V)(V')\right]_n &= \left[\left(I - J\left(DF_s(\overline{U}_0)\right)\right)(V')\right]_n - \left[JD^2F_s(\overline{U}_0)(s\Delta\overline{U} + V)(V')\right]_n \\ &= -J_n DQ_n(\overline{U}_0)(V') - \left[J\left(D^2F_s(\overline{U}_0)(s\Delta\overline{U} + V, V')\right)\right]_n. \end{aligned}$$

Now using (21) we get that

$$\left[DT_s(\overline{U}_s + V)(V')\right]_n = -J_n \left(DQ_n(\overline{U}_0 + s\Delta\overline{U} + V)(V') - (\pi n)^2 \left((s\Delta\overline{d} + d) v_n' + d' (s \underbrace{\Delta\overline{u}_n}_{=0} + v_n) \right) \right).$$

Using the same bounds as for (34) and (35) we can set

$$Z_n = |J_n| \left(\Theta_n^q(\overline{u}) r + s\Theta_n^q(\Delta\overline{u}) r + \widetilde{DQ}_n^q(K) r^2 + \frac{(\pi n)^2}{\omega_n^q} \left(s|\Delta\overline{d}| r + \frac{2r^2}{\rho} \right) \begin{pmatrix} 1 \\ 1 \\ 1 \end{pmatrix} \right).$$

3.7.3 Case $n \geq m$

We still have

$$\left[DT_s(\overline{U}_s + V)(V')\right]_n = -J_n \left(DQ_n(\overline{U}_0 + s\Delta\overline{U} + V)(V') - (\pi n)^2 \left((s\Delta\overline{d} + d)v'_n + d'v_n\right)\right),$$

but here we bound the convolution products in DQ_n using Lemma 3 to get, for all $n \geq M$,

$$\left|\left[DT_s(\overline{U}_s + V)(V')\right]_n\right| \leq |J_n| \left(\frac{1}{2}\frac{\alpha_M^q(K)}{\omega_n^q}\left(\|\overline{u}\|_q r + s\|\Delta\overline{u}\| r + r^2\right)\begin{pmatrix}\lambda_1\\ \lambda_1\\ \lambda_2\end{pmatrix} + \frac{(\pi n)^2}{\omega_n^q}\left(s|\Delta\overline{d}|r + \frac{2r^2}{\rho}\right)\begin{pmatrix}1\\1\\1\end{pmatrix}\right).$$

Then we set

$$\hat{Z}_M = |J_M| \left(\frac{1}{2}\frac{\alpha_M^q(K)}{\omega_M^q}\left(\|\overline{u}\|_q r + s\|\Delta\overline{u}\| r + r^2\right)\begin{pmatrix}\lambda_1\\ \lambda_1\\ \lambda_2\end{pmatrix} + \frac{(\pi M)^2}{\omega_M^q}\left(s|\Delta\overline{d}|r + \frac{2r^2}{\rho}\right)\begin{pmatrix}1\\1\\1\end{pmatrix}\right),$$

and since the terms of $|J_n|$ and $(\pi n)^2 |J_n|$ are decreasing for $n \geq \max\left(\sqrt{\frac{r_1}{\pi^2 d}}, \sqrt{\frac{r_2}{\pi^2 d}}\right)$ (≈ 11 with the values of the parameter taken here, m is always taken such that $2m - 1 > 11$), we can set, for all $n \geq M$,

$$Z_n = \hat{Z}_M \frac{\omega_M^q}{\omega_n^q}. \tag{36}$$

Notice that (36) is what allows us to check the hypotheses of Theorem 3 with finite computations so it is really crucial for the proof, and we are able to do this thanks to the fact that the terms of $|J_n|$ are decreasing, which happens because the magnitude of the eigenvalues of the linear part of f are growing in $(\pi n)^2$. In fact, we would have (36) for every system whose equations can be written as the sum of a linear operator with eigenvalues of increasing magnitude and a non linear polynomial term (in particular for reaction-diffusion systems).

3.8 Explicit computation of the radii polynomials

Now according to Section 2.2.2 and using the bounds Y and Z we got in the two previous sections, we define the radii polynomials. Notice that Y does not depend on r and that Z has linear and quadratic terms in r, so the radii polynomials are all of degree two.

3.8.1 Case $n < m$

Let us set

$$a^{[m]}(s) = |J^{[m]}| \left(\left(\widetilde{DQ}^q\right)^{[m]}(K) + \frac{2}{\rho}(W_2^q)^{[m]} \right),$$

$$\begin{aligned} b^{[m]}(s) &= \left|I^{[m]} - J^{[m]} DF_0^{[m]}(\overline{U}_0^{[m]})\right| (W_1^q)^{[m]} + |J^{[m]}|\tilde{R}^{[m]}(\overline{U}_0) + s\left|J^{[m]}\begin{pmatrix}\left(\Delta\dot{U}\right)^T\\ 0\end{pmatrix}\right|(W_1^q)^{[m]} \\ &+ s|J^{[m]}|\left((\Theta^q)^{[m]}(\Delta\overline{u}) + |\Delta\overline{d}|(W_2^q)^{[m]} + \frac{1}{\rho}\Lambda^{[m]}(\Delta\overline{u})\right) - (W_1^q)^{[m]}, \end{aligned} \tag{37}$$

and

$$c^{[m]}(s) = Y^{[m]}(s).$$

Then we define

$$P_d(r,s) = a_d^{[m]}(s)r^2 + b_d^{[m]}(s)r + c_d^{[m]}(s)$$

and for all $n < m$,

$$P_n(r,s) = a_n^{[m]}(s)r^2 + b_n^{[m]}(s)r + c_n^{[m]}(s).$$

3.8.2 Case $m \leq n < M$

For $m \leq n < 2m-1$, define

$$a_n(s) = |J_n| \left(\widetilde{DQ}_n^q(K) + \frac{2(\pi n)^2}{\rho \omega_n^q} \begin{pmatrix} 1 \\ 1 \\ 1 \end{pmatrix} \right), \tag{38}$$

$$b_n(s) = |J_n| \left(\Theta_n^q(\overline{u}) + s\Theta_n^q(\Delta \overline{u}) \right) + \left(s(\pi n)^2 |\Delta \overline{d}| \, |J_n| \begin{pmatrix} 1 \\ 1 \\ 1 \end{pmatrix} - \begin{pmatrix} 1 \\ 1 \\ 1 \end{pmatrix} \right) \frac{1}{\omega_n^q}, \tag{39}$$

and

$$c_n(s) = Y_n(s).$$

Then for each $m \leq n < M$, we define

$$P_n(r,s) = a_n(s)r^2 + b_n(s)r + c_n(s).$$

3.8.3 Case $n = M$

We have $Y_M = 0$ (from the choice of $M = 2m-1$ as explained in Section 3.6) so $c_M = 0$. Setting

$$a_M(s) = |J_M| \left(\frac{1}{2} \frac{\alpha_M^q}{\omega_M^q} \begin{pmatrix} c_1 \\ c_1 \\ c_2 \end{pmatrix} + \frac{2(\pi M)^2}{\rho \omega_M^q} \begin{pmatrix} 1 \\ 1 \\ 1 \end{pmatrix} \right)$$

and

$$b_M(s) = \left(\frac{1}{2} \alpha_M^q \left(\|\overline{u}\|_q + s \|\Delta \overline{u}\|_q \right) |J_M| \begin{pmatrix} c_1 \\ c_1 \\ c_2 \end{pmatrix} + s(\pi M)^2 |\Delta \overline{d}| \, |J_M| \begin{pmatrix} 1 \\ 1 \\ 1 \end{pmatrix} - \begin{pmatrix} 1 \\ 1 \\ 1 \end{pmatrix} \right) \frac{1}{\omega_M^q}, \tag{40}$$

we can define

$$P_M(r,s) = a_M(s)r^2 + b_M(s)r = a_M(s)r \left(r + \frac{b_M(s)}{a_M(s)} \right).$$

3.8.4 Procedure to find (if possible) $r > 0$ satisfying (14)

To verify hypothesis (14) of Theorem 3, we use Lemma 2. More explicitly we look for $r > 0$ such that, for all $s \in [0,1]$, $P_d(r,s) < 0$ and $P_n(r,s) < 0$ for all $n \leq M$. Notice that the coefficients of the radii polynomials are increasing with s so that it is equivalent to find $r > 0$ such that

$$P_d(r,1) < 0 \quad \text{and} \quad P_n(r,1) < 0, \quad \text{for all } n \leq M. \tag{41}$$

To find such r, we set

$$I_d \overset{\text{def}}{=} \{r > 0 \mid P_d(r,1) < 0\} \quad \text{and} \quad I_n \overset{\text{def}}{=} \{r > 0 \mid P_n(r,1) < 0\}, \quad \text{for all } n \leq M. \tag{42}$$

Then we determine numerically an approximation of

$$I \overset{\text{def}}{=} I_d \cap \left(\bigcap_{n=0}^{M} I_n \right). \tag{43}$$

If $I \neq \emptyset$, we choose $r \in I$, and check (41) rigorously, by computing the coefficients of the radii polynomials with $s = 1$ using interval arithmetic. We see in Section 4.1 why it is reasonable to hope that such r exists, provided the parameters Δ_s, m and q are chosen carefully.

4 Optimization of the parameters

4.1 Optimal choice of the parameters m and Δ_s

Recall that the parameter m controls the dimension (which equals $3m$) of the finite dimensional Galerkin projection given by (17), and from (8), the parameter Δ_s is used to define a predictor $\hat{U}_0 = \overline{U}_0 + \Delta_s \dot{U}_0$ whose value serves as an initial point for Newton's method to get a corrector $\overline{U}_1$. The value of Δ_s represents roughly the arc length of curve we are covering in one predictor-corrector step, hence the name *pseudo-arclength* continuation. Since $\Delta\overline{U} = \overline{U}_1 - \overline{U}_0$, if Δ_s is not so large, then its value should be close to the length $\|\Delta\overline{U}\|$ of the segment $[\overline{U}_0, \overline{U}_1]$. Hence, studying Δ_s is roughly the same as studying the length of $\Delta\overline{U}$.

The optimal strategy aims at maximizing the pseudo-arclength parameter Δ_s to prove existence of long pieces of solution curve in one predictor-corrector step (as explained in Section 2.1) while taking m as small as possible in order to minimize the computational cost. However, the fact that we are looking for an r verifying the hypotheses of Theorem 3 (which is equivalent to find $r > 0$ for which every radii polynomial is negative) leads to some constraints.

Let us now remark that for a quadratic polynomial of the form $P(r) = ar^2 + br + c$, if $a > 0$, $b < 0$ and $c > 0$ is small enough (precisely $c < \frac{b^2}{4a}$), then there is an interval $[r_{min}, r_{max}] \subset (0, \infty)$ such that for all $r \in [r_{min}, r_{max}]$, $P(r) < 0$. Based on this fact, let us study in details the coefficients of each radii polynomial to see how to choose m and Δ_s optimally. Since we showed in Section 3.8 that we could bound the polynomials letting $s = 1$, we always set from now $s = 1$.

4.1.1 Case $n < m$

Recall the definition of the coefficients $a^{[m]}$, $b^{[m]}$ and $c^{[m]}$ of the radii polynomials for the case $n < m$. First notice that each component of $a^{[m]}$ and $c^{[m]}$ is positive. In the definition of $b^{[m]}$, the first two terms are very small (the first by definition of J, and the second provided m is not too small, which will always be the case), and the next two can be made as small as needed (and so $b^{[m]}$ will be negative) by taking Δ_s small enough. $c^{[m]}$ can also be made very small by taking Δ_s small (see Section 3.6.1). Hence we can expect each set I_n (for $n < m$) defined in Section 3.8 to be non empty if Δ_s is small enough (the same is true for I_d).

4.1.2 Case $m \leq n < M$

Recall the definition in Section 3.8.2 of the coefficients a_n, b_n and c_n of the radii polynomial $P_n(r)$ for the case $m \leq n < M$. According to the previous section, Δ_s should not be too large and hence here again c_n should be small. Also, the predominant term of b_n in (39) is $|J_n|\,\Theta_n^q(\overline{u})$ which decreases to 0 as n grows, so taking m large enough should allow us to have b_n negative for $n \geq m$ and thus, recalling (42), we can expect that $I_n \neq \emptyset$ (for $m \leq n < M$).

4.1.3 Case $n = M$

The situation in the case $n = M = 2m - 1$ is the same as above except that the expression of b_M in (40) is different, with m large enough we can expect I_M to be non empty.

4.1.4 Algorithm to choose Δ_s and m optimally

Let us now present an algorithm to chose Δ_s and m optimally. Given $\overline{U}_0$, $\dot{U}_0$, Δ_s and m,

1. Compute $\overline{U}_1$, $\dot{U}_1$ and I given by (43);
2. If for some $n < m$ $I_n = \emptyset$, take Δ_s smaller and go back to Step 1;
3. If for some $m \leq n \leq M$ $I_n = \emptyset$, take m larger and go back to Step 1;
4. If $I = \emptyset$, take Δ_s smaller and go back to Step 1;
5. Start a new predictor-corrector step from $\overline{U}_1$ and $\dot{U}_1$ with Δ_s larger and m smaller.

The fact that we try to increase Δ_s and decrease m after each successful step is not optimal. We indeed observed numerically that the process often failed. In fact we noticed that the value of $\max I$ has to reach some threshold before Δ_s could be increased successfully. Similarly d has to reach some other threshold before m could be decreased successfully. In practice we only try to increase Δ_s or decrease m if those thresholds are reached.

Note that we want to change the value of m along the process while conserving the smoothness property of the global curve. The important fact is to have exactly the same function F_s given by (10) at the end of one piece of curve and at the start of the next, that is $F_1^{(0)} = F_0^{(1)}$ with the notations of Section 2.3, and this even when we change the value of m between the two. Let us denote $m^{(0)}$ (resp. $m^{(1)}$) the value of m for the first curve (resp. the second). In F_s, only E_s changes with m. Hence, we only need to check that $E_1^{(0)} = E_0^{(1)}$. Remember that $\overline{U}_s$ and $\dot{U}_s$ are constructed from finite dimensional vectors and completed with zeros. In fact, $E_1^{(0)}(U) = \left(U^{[m^{(0)}]} - \overline{U}_1^{[m^{(0)}]}\right) \cdot \dot{U}_1^{[m^{(0)}]}$ and $E_0^{(1)}(U) = \left(U^{[m^{(1)}]} - \overline{U}_1^{[m^{(1)}]}\right) \cdot \dot{U}_1^{[m^{(1)}]}$. If we increase m, that is $m^{(1)} > m^{(0)}$, the last $m^{(1)} - m^{(0)}$ frequencies of $\dot{U}_1^{[m^{(1)}]}$ $\left(\text{that is } \left[\dot{U}_1\right]_n, \text{ for } n \in \{m^{(0)} + 1, \ldots, m^{(1)}\}\right)$ are zeros and hence $E_1^{(0)}$ is equal to $E_0^{(1)}$. Decreasing m, that is $m^{(1)} < m^{(0)}$, requires a bit of care since the last frequencies of $\dot{U}_1^{[m^{(0)}]}$ are not necessarily zero. Hence we have to make an intermediate step. Let us denote $\overline{U}_0^{[m^{(0)}]}$ the last point we have and $\dot{U}_0^{[m^{(0)}]}$ a tangent vector at this point. From there, we make a new predictor-corrector step with m equal to $m^{(0)}$, get a point $\overline{U}_1^{[m^{(0)}]}$ and then compute $\dot{U}_1^{[m^{(0)}]}$. Before doing the proof of this portion of curve, we set the $m^{(0)} - m^{(1)}$ frequencies of $\overline{U}_1^{[m^{(0)}]}$ and $\dot{U}_1^{[m^{(0)}]}$ to zero. Then we are able to decrease m at the next step while having exactly the same F_s at the connecting point.

4.2 Optimal choice of the decay rate parameter q

In light of Lemma 1, computing steady state of (1) with Neumann boundary conditions is equivalent to find $U \in \Omega_q$ such that $f(U) = 0$, and that for any fixed $q > 1$. Hence, it seems legitimate to investigate which decay rate q is optimal. The weight ω_n^q defined in (4) depends on q and it influences the value of the norm $\|\cdot\|_q$ and the theoretical bounds of Lemma 3. Since the value of q has a major impact on the radii polynomials, it influences strongly the values of the parameters Δ_s and m used for the proof, and therefore it influences the computational time required to perform the proofs. As one can see in Table 2, depending on the value of q,

the computational costs required to prove the red branches of Figure 10(a) and Figure 10(c) can change drastically. In Figure 7, one can see how q influences the values of Δ_s and m while performing the algorithm of Section 4.1.4 along the first bifurcation branch presented in red in Figure 10(a), and along the first part of the second bifurcation branch presented in red in Figure 10(c). What we see with these comparisons is that, on the red branch of Figure 10(a),

q	Red branch of Figure 10(a)	Red branch of Figure 10(c)
1.2	515	528
1.5	321	393
2	276	408
3	460	2256

Table 2: Computational cost (in seconds), as a function of the decay rate parameter q, required to compute the radii polynomials and find an $r > 0$ at which they are all simultaneously negative. These computations were done without interval arithmetic.

taking q smaller allows using a greater Δ_s but at the expense of a greater m. Hence, a better compromise seems to be somewhere between $q = 1.5$ and $q = 2$. But it seems that when d becomes small, it could also be better to take q smaller in order to use a smaller m (see the case $q = 3$ on Figure 7(d)). Let us see how this evolves when d becomes even smaller. Note that we were able to get the rigorous data (for different values of q) of Table 2 and of Figure 7 because the rigorous computations of the concerned branches did not take too long. However for some other curves, the proof takes much longer, mainly because d gets smaller and hence m must be taken larger for the coefficients b_M of the last radii polynomial (40) to be negative. On the other hand, it only takes one point along the branch to determine, given q, which value of m should be taken in order to make b_M negative. Also, the cost of the proof decreases linearly with Δ_s but increases quadratically with m, so it seems fair to chose q according to m only and independently of Δ_s for those branches where m has to be taken large. In Figure 8(a), we present some non rigorous results concerning the second part of the second branch. Although non rigorous, these results helps understanding the role played by q for the computational cost of the method. We can see in Figure 8(c) that as the diffusion parameter d decreases, the optimal decay rate q becomes smaller as well. That can be explained by the fact that the coefficient b_M of the last radii polynomial is non negative if $M = 2m - 1$ is taken too small. A necessary condition for b_M to be negative is roughly the following

$$\frac{\alpha_M^q \left\|u\right\|_q}{d(\pi M)^2} < \text{some constant},$$

which shows why M has to be taken larger when d becomes smaller. But to understand the impact of q, we have to detail how the values of α_M^q and $\left\|u\right\|_q$ evolve with q. For this let us recall the definitions of $\left\|\cdot\right\|_q$ in (5) and of α_M^q in (24) and let us look at the shape of the solution u. For instance, we see on Figure 9(b) that on the first branch the solutions are almost sinusoids of period 2 and hence $\left\|u\right\|_q \approx \max\left(\left|u_0\right|_\infty \omega_0^q, \left|u_1\right|_\infty \omega_1^q\right) = \max\left(\left|u_0\right|_\infty, \left|u_1\right|_\infty\right)$. Hence, taking q smaller does not decrease the value of $\left\|\cdot\right\|_q$, but it increases slightly α_M^q, and then finally leads to a greater m. However, when d becomes smaller, the high frequencies in the solutions are more and more important. Thus $\left\|u\right\|_q$ involves $\left|u_n\right|_\infty \omega_n^q$ for some $n > 1$ and hence taking q smaller decreases significantly the value of $\left\|\cdot\right\|_q$ and therefore the value of $\alpha_M^q \left\|u\right\|_q / d\pi^2$. This allows taking a smaller m, provided that q is not too small. Indeed, $\alpha_M^q \underset{q\to 1}{\sim} \frac{4}{q-1}$ increases more than $\left\|u\right\|_q$ decreases when q gets close to 1, which explains why the optimal value of q seems not to

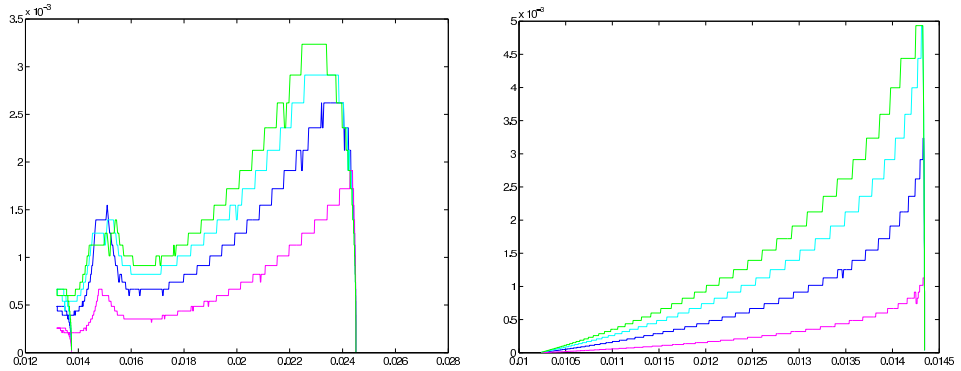

(a) Values of Δ_s along the first branch

(c) Values of Δ_s along the second branch.

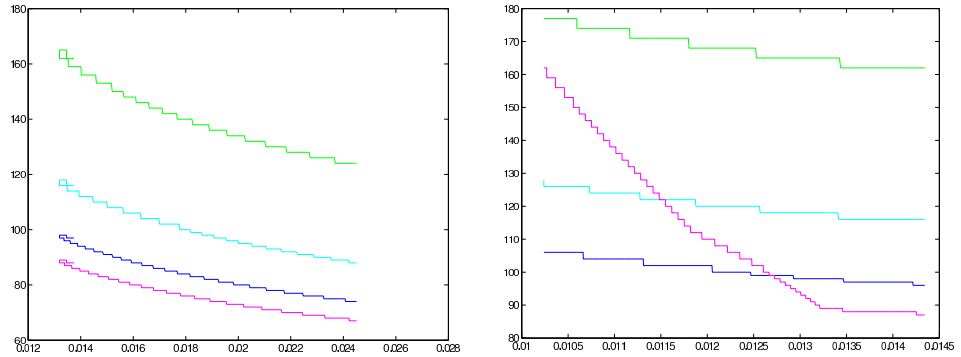

(b) Values of m along the first branch.

(d) Values of m along the second branch

Figure 7: Influence of the decay rate parameter q on the parameters Δ_s and m, accordingly to the Algorithm of Section 4.1.4. **On the left:** results for the branch in red of Figure 10(a). **On the right:** results for the branch in red of Figure 10(c). Green corresponds to $q = 1.2$, cyan corresponds to $q = 1.5$, blue corresponds to $q = 2$ and magenta corresponds to $q = 3$.

go below 1.3. One can see in Figure 8(c) that when d is really small, the value of m is far much smaller with $q = 1.2$ than with $q = 2$. This is a significant improvement, especially in terms of the computational cost which evolves in m^3. Actually, we did some computation, and the cost of the proof to do part of a branch for small d is about 10 times faster with $q = 1.3$ than with $q = 2$. This brings us to the conclusion that the new estimates introduced in Section 3.5 for $q < 2$ can be quite useful. Actually, they allowed proving parts of some branches in Figure 8(a) which we would not have been able to do with $q = 2$.

5 Proofs of two main results of Section 1

5.1 Proof of Theorem 1

Recall (7) and fix $\rho = 10$. Set $K = 10^4$ in the bounds of Lemma 3 and set $K = 3M$ in those of Lemma 4. Set the multiplicative coefficient used to change Δ_s equal to $\frac{10}{9}$ and the one used to change m equal to 1.02. That means that in the algorithm of Section 4.1.4, taking Δ_s larger means setting $\Delta_s = \frac{10}{9}\Delta_s$, taking Δ_s smaller means setting $\Delta_s = \frac{9}{10}\Delta_s$, taking m larger means setting $m = \lfloor 1.02m \rfloor$ and taking m smaller means setting $m = \lfloor m/1.02 \rfloor$. We proved that in a small tube (whose size is given by r) of each portion of curve represented in Figure 1 between two bifurcation points, there exists a unique smooth curve representing exactly one steady states of (1). Note that the method cannot prove that those curves really reach the bifurcation points, but we can virtually go as close as we want to those bifurcation points, the only limit being the

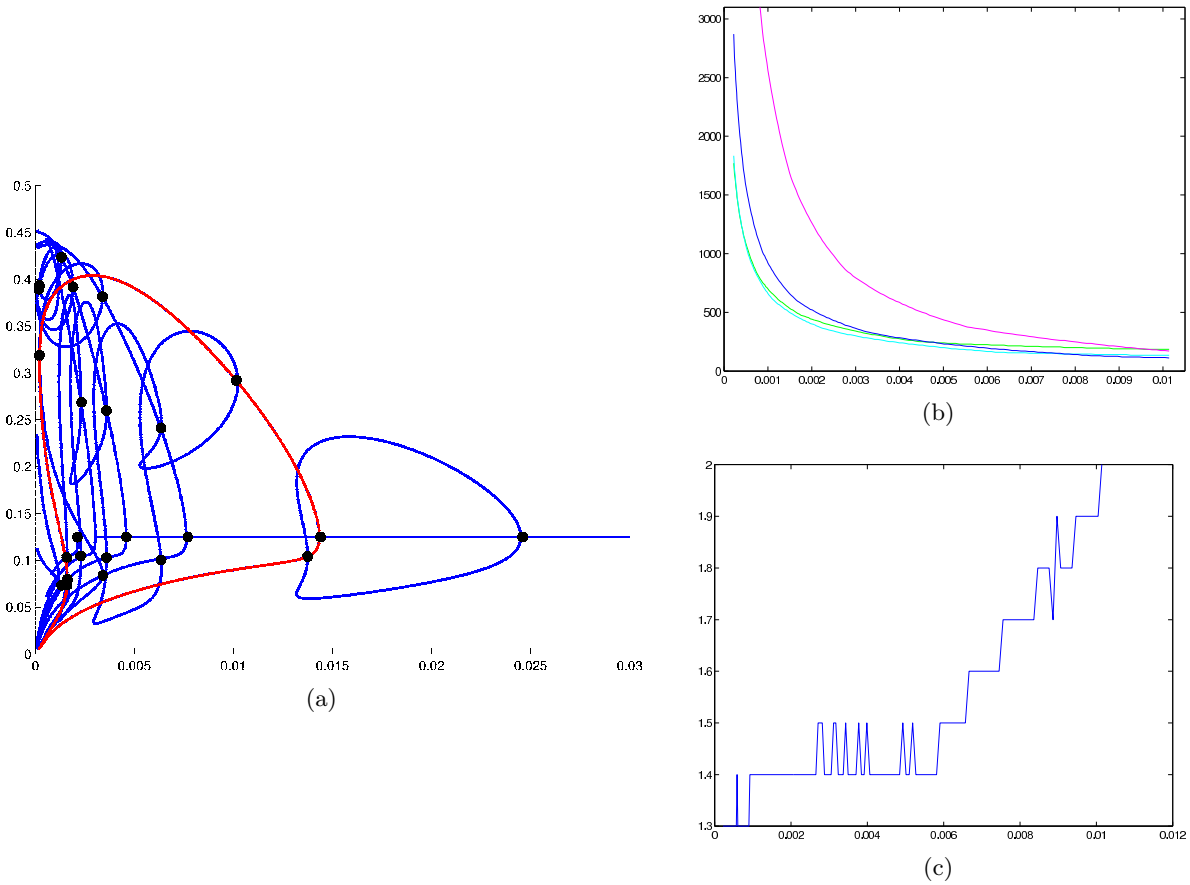

(a) (b) (c)

Figure 8: (a) A more complete (non rigorous) bifurcation diagram of steady states of (1). (b) Values of m along the branch for different q. Green corresponds to $q = 1.2$, cyan corresponds to $q = 1.5$, blue corresponds to $q = 2$ and magenta corresponds to $q = 3$. (c) Best values of q to use along the branch as a function of d in order to get m as small as possible.

computational cost. On the other hand, applying the result of Corollary 2, we can conclude that along the rigorously computed smooth branches, there are no secondary bifurcation of steady states. In Table 2, Figure 7 and Figure 9, one has some example of the parameters used, the running time required to compute the branches and some spatial representations of solutions on different branches. □

5.2 Proof of Corollary 1

Consider one portion of branch we have proven. We have the existence of a smooth function $\tilde{U}$ (defined on $[0, 1]$) parametrising our portion of curve, and we know that it lies in a *tube* of radius r around our numerical solution. So we know the initial point and the final point with a precision of r in $\|\cdot\|_q$. In particular, if $\overline{d}_{in}$ (respectively $\overline{d}_f$) is the numerical value of d from which the branch starts (respectively at which the branch finishes) then there exists a $\tilde{d}_{in}$ in $\left[\overline{d}_{in} - \frac{r}{\rho}, \overline{d}_{in} + \frac{r}{\rho}\right]$ and a $\tilde{d}_f$ in $\left[\overline{d}_f - \frac{r}{\rho}, \overline{d}_f + \frac{r}{\rho}\right]$ such that $\tilde{U}_d(0) = \tilde{d}_{in}$ and $\tilde{U}_d(1) = \tilde{d}_f$. Thus, if the branch we are considering is such that

$$\overline{d}_{in} - \frac{r}{\rho} > 0.006 \quad \text{and} \quad \overline{d}_f + \frac{r}{\rho} < 0.006,$$

or reversely

$$\overline{d}_{in} + \frac{r}{\rho} < 0.006 \quad \text{and} \quad \overline{d}_f - \frac{r}{\rho} > 0.006$$

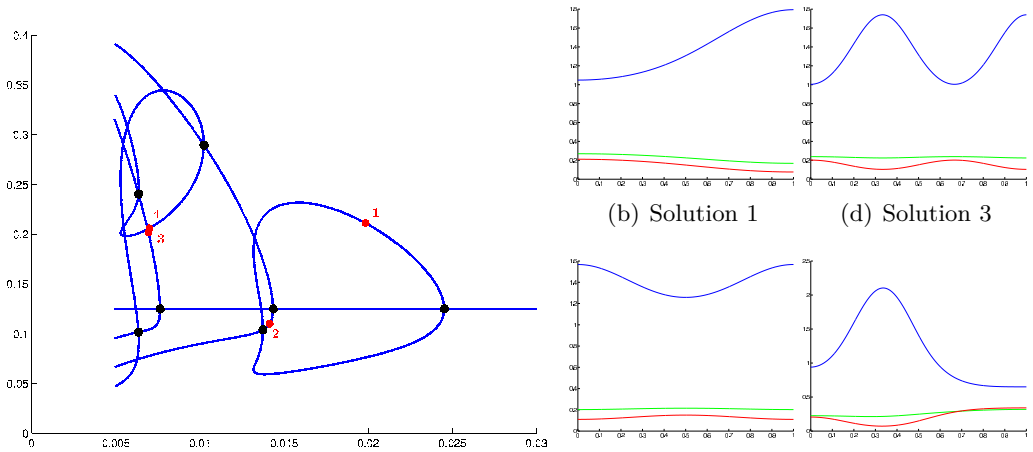

(a) The chosen steady states

(b) Solution 1

(c) Solution 2

(d) Solution 3

(e) Solution 4

Figure 9: Spatial representation of some steady states of Theorem 1 with x blue, y green and z red.

then the intermediate value theorem yields the existence of an s in $(0,1)$ such that $\tilde{U}_d(s) = 0.006$. Notice that if $d = 0.006$ is too close to $\overline{d}_{in}$ or $\overline{d}_f$ for those hypothesis to be satisfied, you just have to consider several consecutive portions of curve rather than a single one. On the diagram we proved, there are eleven such portions (see Figure 2). To complete our proof, we need to check that each solution is different from one another, and we are able to do this because the radius r we get in our proofs are small enough. Remember that what we are representing on our bifurcation diagram is the value of z at 0 and that

$$\tilde{z}(0) = \frac{\tilde{z}_0}{2} + \sum_{n=1}^{\infty} \tilde{z}_n.$$

Besides we know that $\left\|\tilde{U}(s) - \overline{U}_s\right\|_q < r$ so

$$\left|\tilde{z}(0) - \left(\frac{\overline{z}_0}{2} + \sum_{n=1}^{m-1} \overline{z}_n\right)\right| < \frac{r}{2} + \sum_{n=1}^{\infty} \frac{r}{n^q}.$$

In fact, the quantity $\dfrac{\overline{z}_0}{2} + \displaystyle\sum_{n=1}^{m-1} \overline{z}_n$ is the one we represented on the diagram, and so the error we did by using this representation is bounded by

$$\varepsilon_r \overset{\text{def}}{=} r\left(\frac{1}{2} + \sum_{n=1}^{\infty} \frac{1}{n^q}\right).$$

With the value of q we used and the r we got, those ε_r were always smaller than 10^{-4} and hence the error we made are in fact lying in thickness of the line on the diagram, so we are sure that we have eleven different solutions. □

A Appendix

A.1 Sharper estimates for $q^*(M) \leq q < 2$

What we have already proven in the proof of Proposition 1 in (31) is that, for all $q \in [q^*(M), 2)$ and $n \geq M$

$$\Psi_n^q \leq 2 + 4\sum_{k=1}^{\infty} \frac{1}{k^q} + \chi_n(q),$$

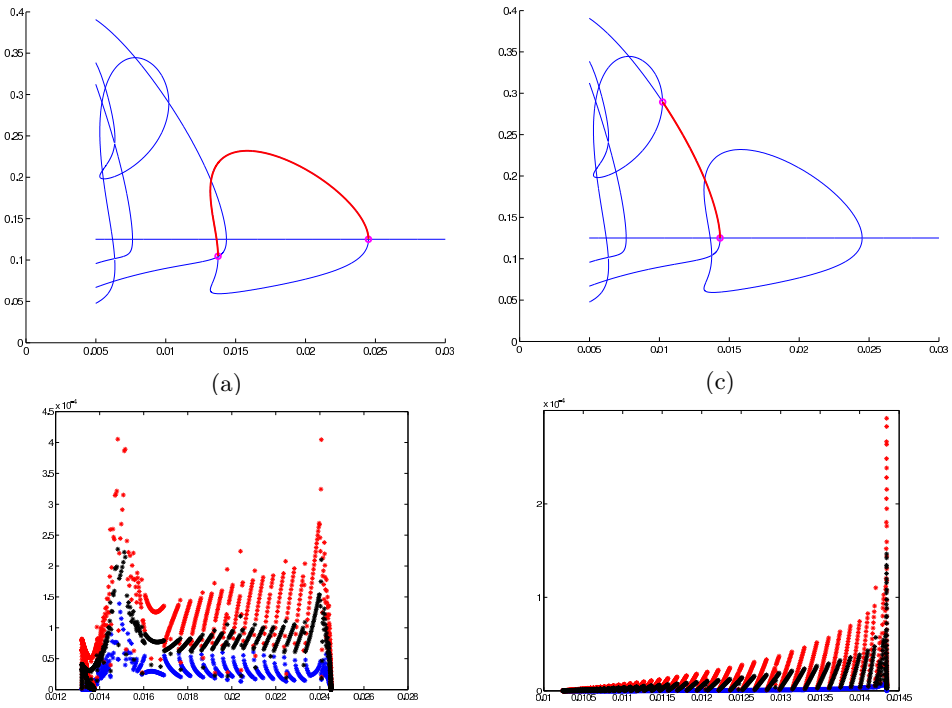

Figure 10: Proofs of the branches in red with $q = 2$. **On the left:** The radius of the *tubes* in which we proved the existence of a unique portion of curve are between $2.1e^{-4}$ and $4.7e^{-8}$. **On the right:** The radius of the *tubes* in which we proved the existence of a unique portion of curve are between $2.2e^{-4}$ and $1.7e^{-8}$. For parts (b) and (d), the values of $\min(I)$ are in blue and the values of $\max(I)$ are in red along the branch. In black the values of r used for the rigorous verification using interval arithmetic.

and since we needed a uniform bound, we took $2 + 4\sum_{k=1}^{\infty} \frac{1}{k^q} + \chi_M(q)$. Since $\lim_n \chi_n(q) = 0$, we would like to take m and hence $M = 2m - 1$ larger to improve the estimate, but the point of getting a sharp estimate is to allow us to take m smaller, so this does not really make sense. However, there is a way to rigorously compute a bound that is almost optimal, without increasing m. Let $\varepsilon > 0$, $\exists n_0$, $\forall n \geq n_0$, $\chi_n(q) < \varepsilon$ and since $\chi_n(q)$ is deceasing such n_0 can be computed numerically and rigorously using interval arithmetic. Then we have that, for all $n \geq M$

$$\Psi_n^q \leq \max\left(2 + 4\sum_{k=1}^{K} \frac{1}{k^q} + \frac{4}{(q-1)K^{q-1}} + \varepsilon, \max_{M \leq n < n_0}\left(2 + 2\sum_{k=1}^{K} \frac{1}{k^q} + \frac{2}{(q-1)K^{q-1}} + \sum_{k=1}^{n-1} \frac{n^q}{k^q\,(n-k)^q}\right)\right),$$

the max being computed rigorously using interval arithmetic. We can have a bound as sharp as we want by taking ε small, but at the expense of some computational cost which is in $\mathcal{O}(n_0^2)$. Indeed, when q goes to 2, $\chi_n(q)$ is equivalent to $\frac{q}{2-q}\frac{1}{\lfloor \frac{n}{2} \rfloor^{q-1}}$ and hence $n_0 \approx \left(\frac{2q}{2-q}\frac{1}{\varepsilon}\right)^{\frac{1}{q-1}}$.

A.2 Sharper uniform bounds for $s \in [0, 1]$ for Y

To prove that $\tilde{T}$ is a uniform contraction, we have in Section 3.6 to bound uniformly in s terms of the form $g(s) \stackrel{\text{def}}{=} |\alpha s^2 + \beta s + \gamma|$ for s in $[0, 1]$. We did that the simplest way, using triangular inequality to say that

$$\begin{aligned} g(s) &\leq |\alpha| s^2 + |\beta| s + |\gamma| \\ &\leq |\alpha| + |\beta| + |\gamma|, \quad \forall s \in [0, 1]. \end{aligned}$$

However, given the expression of g, we can get a better bound which depends on whether the apex of g is between 0 and 1 or not. More explicitly,

$$\forall s \in [0,1],\ g(s) \leq \begin{cases} \max\left(|g(0)|, |g(1)|\right) = \max\left(|\gamma|, |\alpha+\beta+\gamma|\right), & \text{if } -\dfrac{\beta}{2\alpha} \notin [0,1], \\ \max\left(|g(0)|, \left|g\left(\dfrac{-\beta}{2\alpha}\right)\right|, |g(1)|\right) = \max\left(|\gamma|, \left|-\dfrac{\beta^2}{4\alpha}+\gamma\right| |\alpha+\beta+\gamma|\right), & \text{else.} \end{cases}$$

References

[1] Yukio Kan-on and Masayasu Mimura. Singular perturbation approach to a 3-component reaction-diffusion system arising in population dynamics. *SIAM J. Math. Anal.*, 29(6):1519–1536 (electronic), 1998.

[2] Rui Peng and Mingxin Wang. Pattern formation in the Brusselator system. *J. Math. Anal. Appl.*, 309(1):151–166, 2005.

[3] Michael G. Crandall and Paul H. Rabinowitz. Bifurcation from simple eigenvalues. *J. Functional Analysis*, 8:321–340, 1971.

[4] Paul H. Rabinowitz. Some global results for nonlinear eigenvalue problems. *J. Functional Analysis*, 7:487–513, 1971.

[5] Masato Iida, Masayasu Mimura, and Hirokazu Ninomiya. Diffusion, cross-diffusion and competitive interaction. *J. Math. Biol.*, 53(4):617–641, 2006.

[6] A.M. Turing. The chemical basis of morphogenesis. *Phil. Trans. R. Soc. Lond. B*, 237:37–72, 1952.

[7] Herbert Amann. Nonhomogeneous linear and quasilinear elliptic and parabolic boundary value problems. In *Function spaces, differential operators and nonlinear analysis (Friedrichroda, 1992)*, volume 133 of *Teubner-Texte Math.*, pages 9–126. Teubner, Stuttgart, 1993.

[8] Y. S. Choi, Roger Lui, and Yoshio Yamada. Existence of global solutions for the Shigesada-Kawasaki-Teramoto model with weak cross-diffusion. *Discrete Contin. Dyn. Syst.*, 9(5):1193–1200, 2003.

[9] Yuan Lou, Wei-Ming Ni, and Yaping Wu. On the global existence of a cross-diffusion system. *Discrete Contin. Dynam. Systems*, 4(2):193–203, 1998.

[10] Hirofumi Izuhara and Masayasu Mimura. Reaction-diffusion system approximation to the cross-diffusion competition system. *Hiroshima Math. J.*, 38(2):315–347, 2008.

[11] Jan Bouwe van den Berg, Jean-Philippe Lessard, and Konstantin Mischaikow. Global smooth solution curves using rigorous branch following. *Math. Comp.*, 79(271):1565–1584, 2010.

[12] Sarah Day, Jean-Philippe Lessard, and Konstantin Mischaikow. Validated continuation for equilibria of PDEs. *SIAM J. Numer. Anal.*, 45(4):1398–1424 (electronic), 2007.

[13] H. B. Keller. *Lectures on numerical methods in bifurcation problems*, volume 79 of *Tata Institute of Fundamental Research Lectures on Mathematics and Physics*. Published for the Tata Institute of Fundamental Research, Bombay, 1987. With notes by A. K. Nandakumaran and Mythily Ramaswamy.

[14] Shui Nee Chow and Jack K. Hale. *Methods of bifurcation theory*, volume 251 of *Grundlehren der Mathematischen Wissenschaften [Fundamental Principles of Mathematical Science]*. Springer-Verlag, New York, 1982.

[15] Marcio Gameiro and Jean-Philippe Lessard. Analytic estimates and rigorous continuation for equilibria of higher-dimensional PDEs. *J. Differential Equations*, 249(9):2237–2268, 2010.